Influence of Hydrogen Ion Activity and General Acid–Base Catalysis on the Rate of Decomposition of Hydrogen Peroxide by a Novel Nonaggregating Water-Soluble Iron(III) Tetraphenylporphyrin Derivative

Matthias F. Zipplies, William A. Lee, and Thomas C. Bruice*

Contribution from the Department of Chemistry, University of California at Santa Barbara, Santa Barbara, California 93106. *Received October 15, 1985*

Abstract: The synthesis and characterization of 5,10,15,20-tetrakis(2,6-dimethyl-3-sulfonatophenyl)porphyrin (**3**) and its iron(III) complex (**3**-Fe^{III}) are described. Both **3** and **3**-Fe^{III} hydrate exist as a mixture of atropisomers due to the dissymmetry of the four 2,6-dimethyl-3-sulfonatophenyl substituents. Spectrophotometric titrations of the atropisomer mixture at a number of wavelengths establish that the observed changes in absorbance with change in pH fit (±0.05 and ±0.08 pH units) to the equation for the titration of a single monobasic acid (**3**-$Fe^{III}(H_2O)_2 \rightleftarrows$ **3**-$Fe^{III}(H_2O)(OH) + H^+$; $pK_a = 7.25$). Ligation of a second hydroxyl group (i.e., **3**-$Fe^{III}(H_2O)(OH) \rightleftarrows$ **3**-$Fe^{III}(HO)_2 + H^+$) is not seen on titration to pH 14. The observation of a single pK_a shows that the various atropisomers possess the same acidity. Therefore, oxyligands attached to the iron(III) moiety of the various atropisomers are under the same electronic influence. The same conclusion is reached from electrochemical measurements. The water-soluble aquo-ligated **3**-Fe^{III} does not show spectral evidence for self-association nor μ-oxo dimer formation. The rate constants for the reaction of the iron(III) porphyrin with hydrogen peroxide as a function of pH (1 to 12) and buffer concentrations have been determined by employing 2,2′-azinobis(3-ethylbenzthiazoline)sulfonic acid(6) (ABTS) as a trap for the intermediate higher valent iron–oxo porphyrin species. The reactions were monitored with time at an absorbance maximum (660 nm) of the radical product $ABTS^{\cdot+}$. The oxidation of hydrogen peroxide to oxygen competes with oxidation of ABTS, and the former reaction is favored with increasing pH. The log of the apparent second-order rate constants for the buffer-insensitive reaction of hydrogen peroxide with the iron(III) porphyrin (k_{1y}) when plotted vs. pH provides a profile which could be fit to the appropriate rate expression for the three following reactions: **3**-$Fe^{III}(H_2O)_2 + H_2O_2$; **3**-$Fe^{III}(H_2O)(HO) + H_2O_2$; and **3**-$Fe^{III}(H_2O)(HO) + HOO^-$. From the kinetics, the composition of the three transition states is defined. The various kinetically equivalent transition-state structures for each of the three reactions are identified and discussed. Of the various buffers employed ($ClCH_2CO_2H/ClCH_2CO_2^-$, $CH_3CO_2H/CH_3CO_2^-$, 2,4,6-collidine/2,4,6-collidine·H^+, $H_2PO_4^-/HPO_4^{2-}$ and HCO_3^-/CO_3^{2-}) catalysis was seen only by the collidine buffer. From the dependence of the buffer rates upon buffer concentration and pH it has been established that the collidine free base and its conjugate acid enter into reactions which are first order in the components: **3**-$Fe^{III}(H_2O)(HO) + H_2O_2$ + collidine and **3**-$Fe^{III}(H_2O)(HO) + H_2O_2$ + collidine·H^+. The free energy of activation for these reactions differs by but 1 kcal M^{-1}. The reactions are considered in terms of general-base and general-acid catalysis of O–O bond scission within **3**-$Fe^{III}(HO)(HOO)$ (and kinetically equivalent structures). Possible mechanisms for the general catalysis are discussed.

The reaction of hydrogen peroxide with ferric porphyrins is of interest with respect to several classes of enzymes. The peroxidases catalyze the oxidation of a variety of compounds by hydrogen peroxide;[1] closely related are the catalases, which promote the decomposition of hydrogen peroxide to oxygen and water.[2] Both enzymes are highly efficient with the formation of the outer-sphere porphyrin–hydrogen peroxide complex probably being the rate-determining step.[1] The cytochrome P-450 enzymes[3] on the other hand are mixed function oxidases which utilize molecular oxygen and NADPH to oxidatively metabolize a large number of different substrates. A mechanistic relation between cytochrome P-450 and the peroxidases has been shown as the former also displays a peroxidatic capability—known as the "peroxide shunt"—by which it can alternatively employ various hydroperoxides as well as peroxyacids as oxidizing agents.[4] It is not quite clear, however, if the way in which hydroperoxides are processed by the P-450 and peroxidase enzymes is the same; nor is it settled if the reactive intermediate formed in the P-450 system via the $NADPH/O_2$ or the hydroperoxide pathway are identical.[4g,h] Common to all three classes of enzymes is their prosthetic group, ferric protoporphyrin(IX). The enzymes differ in the axial ligation of the central iron(III) moiety. A cysteine sulfur provides one axial ligand in the case of cytochrome P-450 whereas an imidazole of a histidine residue is the axial ligand in the case of most peroxidases.

Scheme I

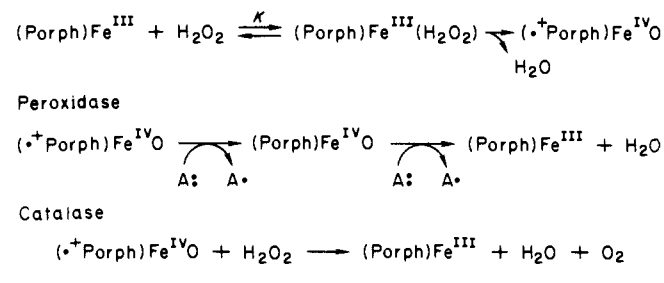

The decomposition of hydrogen peroxide and peroxyacids by iron(III) porphyrins has been examined by several groups.[5]

(1) Dunford, H. B.; Stillman, J. S. *Coord. Chem. Rev.* **1976**, *19*, 187.
(2) Schonbaum, G. R.; Chance, B. In *The Enzymes*, 3rd ed.; Boyer, P. D., Ed.; Academic Press: New York, 1973; Vol. 8C, p 363.
(3) (a) Ullrich, V. *Top. Curr. Chem.* **1979**, *83*, 67. (b) Gunsalus, I. C.; Sligar, S. *Adv. Enzymol. Relat. Areas Mol. Biol.* **1978**, *47*, 1. (c) White, R. E.; Coon, M. J. *Annu. Rev. Biochem.* **1980**, *49*, 315. (d) *Cytochrome P-450*; Sato, R., Omura, T., Eds.; Academic Press: New York, 1978.
(4) (a) Hrycay, E. G.; O'Brien, P. J. *Arch. Biochem. Biophys.* **1971**, *147*, 4. (b) Hrycay, E. G.; O'Brien, P. J. *Arch. Biochem. Biophys.* **1973**, *157*, 7. (c) Kadlubar, K. C.; Morton, K. C.; Ziegler, D. M. *Biochem. Biophys. Res. Commun.* **1973**, *54*, 1255. (d) Hrycay, E. G.; O'Brien, P. J. *Arch. Biochem. Biophys.* **1974**, *160*, 230. (e) Nordblom, G. D.; White, R. E.; Coon, M. J. *Arch. Biochem. Biophys.* **1976**, *175*, 524. (f) Blake, R. C.; Coon, M. J. *J. Biol. Chem.* **1981**, *256*, 12127. (g) McCarthy, M. B.; White, R. E. *J. Biol. Chem.* **1983**, *258*, 9135. (h) Estabrook, R. W.; Martin-Wixtrom, C.; Saeki, Y.; Renneburg, R.; Hildebrandt, A.; Werringloer, J. *Xenobiotica* **1984**, 87.
(5) (a) Euler, H. V.; Josephson, K. *J. Justus Liebigs Ann. Chem.* **1927**, *456*, 111. (b) Kremer, M. L. *Trans. Faraday Soc.* **1965**, *61*, 1453. (c) Kremer, M. L. *Trans. Faraday Soc.* **1967**, *63*, 1208. (d) Gatt, R.; Kremer, M. L. *Trans. Faray Soc.* **1967**, *63*, 721. (e) Brown, S. B.; Dean, T. C.; Jones, P. *Biochem. J.* **1970**, *117*, 741. (f) Portsmouth, D.; Beal, E. A. *Eur. J. Biochem.* **1971**, *19*, 479. (g) Jones, P.; Robson, T.; Brown, S. B. *Biochem. J.* **1973**, *135*, 353. (h) Jones, P.; Prudhoe, K.; Robson, T.; Kelly, H. C. *Biochemistry* **1974**, *13*, 4279. (i) Kelly, H. C.; Davies, D. M.; King, M. J.; Jones, P. *Biochemistry* **1977**, *16*, 3543. (j) Jones, P.; Mantle, D.; Davies, D. M.; Kelley, H. C. *Biochemistry* **1971** *16*, 3974. (k) Hatzikonstantinou, H.; Brown, S. B. *Biochem. J.* **1978**, *174*, 893. (l) Jones, P.; Mantle, D.; Wilson, I. *J. Chem. Soc., Dalton Trans.* **1983**, *161*. (m) Traylor, T. G.; Lee, W. A.; Stynes, D. V. *J. Am. Chem. Soc.* **1984**, *106*, 755.

0002-7863/86/1508-4433$01.50/0

Questions posed, among others, have dealt with the rationale for the high reaction rates observed for the peroxidases (k[rate of compound I formation] = 1.8×10^7 M^{-1} s^{-1})[6] and the mode of oxygen–oxygen bond scission (homolytic vs. heterolytic) in the generation of compound I. On grounds of both enzymatic and model studies, the Scheme I has been proposed.[1,5c,7]

It has been claimed that the mechanisms for the reaction of H_2O_2 with hemin and ferric salts are similar, with the latter even being the better catalyst at low pH.[5b,c] The greater catalatic activity of iron(III) porphyrin at high pH has been attributed to solubilization of the ferric ion by the porphyrin ligand.[5b,c] The rate enhancement brought about by the enzyme vs. the free hemin has been explained by the higher rate of formation (larger equilibrium constant K) of the primary hemin peroxide complex in the enzyme[5b] as well as catalysis by general acids[5g,i,8] and general bases.[5m] The latter hypotheses have received support from the results of the X-ray structure analysis of cytochrome c peroxidase.[9]

All mechanistic studies of ferric porphyrins in water have been complicated by their low solubility in this solvent, their instability with respect to the loss of iron ion at low pH, their tendency to aggregate extensively,[10] and their predilection to dimerize at neutral and basic pH to a μ-oxo-dimer species.[11] Traylor et al.[5m] circumvented these problems by employing methanol as solvent in a study of the reaction of ferric protoporphyrin derivatives with hydrogen peroxide and peracids. Evidence for general base catalysis was presented. The use of the glass electrode to monitor the actual hydrogen ion activity is not feasable in methanol. However, studies of general base and general acid catalysis require a precise knowledge of pH. The ideal solvent for such an investigation is, therefore, water. We report herein an investigation of the pH and buffer base and buffer acid dependence of the reaction of hydrogen peroxide with an iron(III) porphyrin. In line with our ongoing and recent studies[12] directed toward systematic investigations of the dynamics and mechanisms of formation of higher valent metal–oxo porphyrin complexes and their subsequent reactions, we are also interested in extending these studies to aqueous solution.

In order to carry out investigations in water it is desirable to have a nonaggregating, water-soluble iron(III) porphyrin which, as an additional requirement, should not form a μ-oxo dimer. As was shown by Balch and co-workers, substituting all ortho positions of the *meso*-phenyl rings of tetraphenylporphyrin with methyl groups prevents μ-oxo-dimer formation.[13] The ferric complex (**1**-Fe^{III}) of 5,10,15,20-tetrakis(2,6-dimethylphenyl)porphyrin (**I**) meets these criteria. 5,10,15,20-Tetrakis(2,6-dimethyl-4-sulfonatophenyl)porphyrin iron(III) (**2**-Fe^{III}), a hydrophilic derivative of **1**-Fe^{III}, was chosen as a likely candidate for a well-behaved water-soluble iron(III) porphyrin model compound. The photophysical properties of the parent ligand **2** have been reported by Lee et al.[14] However, no satisfactory procedure for the preparation of **1** and **2** nor their characterization has been provided in the aforementioned publication. In this publication we show that the sulfonation of **1** provides a mixture of atropisomers of 5,10,15,20-tetrakis(2,6-dimethyl-3-sulfonatophenyl)porphyrin (**3**). Furthermore, we describe the synthesis and characterization of the iron(III) complex of **3** (i.e., **3**-Fe^{III}) as well as its reactions with hydrogen peroxide as a function of buffer composition and pH.

Results

5,10,15,20-Tetrakis(2,6-dimethyl-3-sulfonatophenyl)porphyrin (3). Sulfonation of [5,10,15,20-tetrakis(2,6-dimethylphenyl)-porphinato]zinc(II) (**1**-Zn^{II}), prepared in analogy to the procedure of Badger,[15] provided a deeply colored microcrystalline material which gave a satisfactory elemental analysis for the nonahydrate of the tetrasodium salt of tetrasulfonated **1**. Both secondary ion

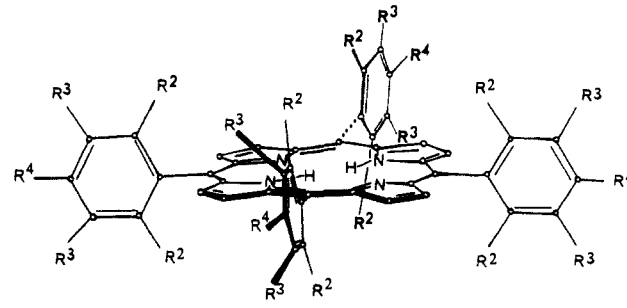

1 : $R^2 = CH_3$; $R^3 = R^4 = H$

2 : $R^2 = CH_3$; $R^3 = H$; $R^4 = SO_3^-$

3 : $R^2 = CH_3$; $R^3 = H$; SO_3^-; $R^4 = H$

4 : $R^2 = R^3 = H$; $R^4 = SO_3^-$

5 : $R^2 = R^4 = CH_3$; $R^3 = H$

mass spectroscopy (SIMS) and laser desorption Fourier transform mass spectroscopy (LDFTMS) confirmed the elemental composition of the compound. In contrast to the claim in the literature,[14] the compound does not possess the structure **2**.

The 300-MHz proton NMR (methanol-d_4) was more complex than expected for the centrosymmetric **2** which has all four sulfonato groups in para positions of the meso phenyl rings. Instead of finding only one singlet for all eight methyl groups, one observes two symmetrical groups (integrating for 12 protons each) of four apparent singlets in the ratio of 1:3:3:1 at δ 2.344, 2.320, 2.292, 2.259 and 1.882, 1.852, 1.823, 1.796, respectively. Apparently the four sulfonato groups are occupying the meta positions of the *meso*-phenyl rings, thus, theoretically, giving rise to a statistical mixture of four atropisomers of 5,10,15,20-tetrakis-(2,6-dimethyl-3-sulfonatophenyl)porphyrin (**3**), which differ in the distribution of these substituents relative to the molecular plane of the porphyrin molecule, i.e., [up, up, up, down]:[up, up, down, down]:[up, down, up, down]:[up, up, up, up] = 4:2:1:1). This phenomenon has been observed, and its implications concerning NMR spectra have been discussed by Walker[16] for simpler tetraphenylporphyrins. Analytical thin-layer reversed-phase chromatography confirmed the presence of at least three products (approximate ratios 5:2:1). Separation of the different isomers by reversed-phase HPLC with the same solvent system was not successful. The isomer mixture of **3** had a typical porphyrin

(6) Loach, P. A.; Calvin, M. *Biochemistry* **1963**, *2*, 361.
(7) Ogura, Y. *Arch. Biochem. Biophys.* **1955**, *57*, 288.
(8) Jones, P.; Suggett, A. *Biochem. J.* **1968**, *110*, 621.
(9) (a) Poulos, T. L.; Freer, S. T.; Alden, R. A.; Edwards, S. L.; Skoglund, U.; Takio, K.; Eriksson, B.; Xuong, N.-H.; Yonetani, T.; Kraut, J. *J. Biol. Chem.* **1980**, *255*, 575. (b) Poulos, T. L.; Kraut, J. *J. Biol. Chem.* **1980**, *255*, 8199.
(10) (a) Brown, S. B.; Dean, T. C.; Jones, P. *Biochem. J.* **1970**, *117*, 733. (b) White, W. I.; Plane, R. A. *Bioinorg. Chem.* **1974**, *4*, 21. (c) Goff, H.; Morgan, L. O. *Inorg. Chem.* **1976**, *15*, 2062. (d) Abraham, R. J.; Evans, B.; Smith, K. M. *Tetrahedron* **1978**, *34*, 1213 and references cited therein.
(11) (a) Sadasivan, N.; Eberspaecher, H. I.; Fuschsman, W. H.; Caughey, W. S. *Biochemistry* **1969**, *8*, 534. (b) Cohen, I. *J. Am. Chem. Soc.* **1969**, *91*, 1980. (c) Fleischer, E. B.; Palmer, J. M.; Srivastava, T. S.; Chatterjee, A. *J. Am. Chem. Soc.* **1971**, *93*, 3162. (d) Pasternak, R. F.; Huber, P. R.; Boyd, P.; Engasser, G.; Francesconi, L.; Gibbs, E.; Fasella, P.; Venturo, G. C.; Hinds, L. de C. *J. Am. Chem. Soc.* **1972**, *94*, 4511. (e) White, W. I. In *The Porphyrins*; Dolphin, D., Ed.; Academic Press: New York, 1979; Vol. VC, Chapter 7. (f) Krishnamurthy, M.; Sutter, J. R.; Hambright, P. *J. Chem. Soc., Chem. Commun.* **1975**, 13.
(12) (a) Powell, M. F.; Pai, E. F.; Bruice, T. C. *J. Am. Chem. Soc.* **1984**, *106*, 3277. (b) Yuan, L.-C.; Bruice, T. C. *J. Am. Chem. Soc.* **1985**, *107*, 512. (c) Lee, W. A.; Bruice, T. C. *J. Am. Chem. Soc.* **1985**, *107*, 513. (d) Yuan, L.-C.; Bruice T. C. *Inorg. Chem.* **1985**, *24*, 986. (e) Lee, W. A.; Calderwood, T. S.; Bruice, T. C. *Proc. Natl. Acad. Sci. U.S.A.* **1985**, *82*, 4301. (f) Yuan, L.-C.; Bruice, T. C. *J. Chem. Soc., Chem. Commun.* **1985**, *868*. (g) Dicken, C. M.; Lu, F.-L.; Nee, M. W.; Bruice, T. C. *J. Am. Chem. Soc.* **1985**, *107*, 5776. (h) Yuan, L.-C.; Bruice, T. C. *J. Am. Chem. Soc.* **1986**, *108*, 1643. (i) Lee, W. A.; Bruice, T. C. *Inorg. Chem.* **1986**, *25*, 131. (j) Calderwood, T. S.; Bruice, T. C. *J. Am. Chem. Soc.* **1985**, *107*, 8272.
(13) Cheng, R.-J.; Latos-Grazynski, L.; Balch, A. L. *Inorg. Chem.* **1982**, *21*, 2412.
(14) Lee, W. A.; Graetzel, M.; Kalyanasundaram, K. *Chem. Phys. Lett.* **1984**, *107*, 308.
(15) Badger, G. M.; Jones, R. A.; Laslett, R. L. *Aust. J. Chem.* **1964**, *17*, 1028.
(16) Walker, F. A. *Tetrahedron Lett.* **1971**, 4949.

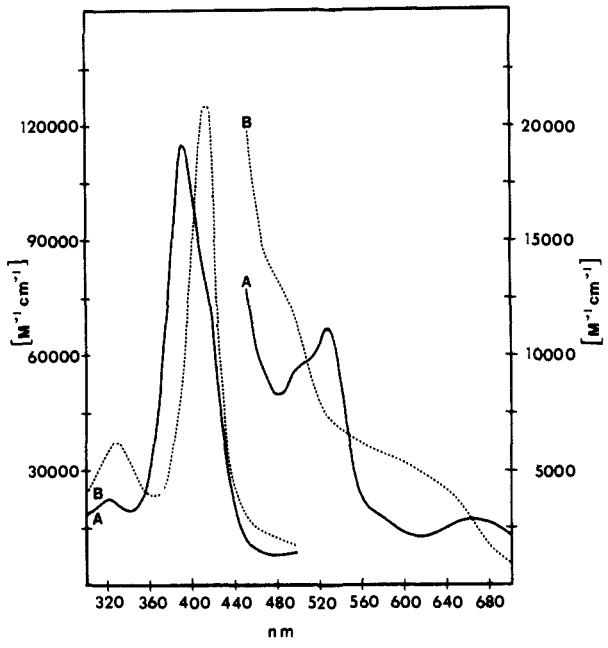

Figure 1. Absorption spectra of 3-$Fe^{III}(H_2O)_2$ (A, pH 3.25, KH-phthalate buffer) and 3-$Fe^{III}(H_2O)OH$ (B, pH 9.70, HCO_3^-/CO_3^{2-} buffer).

absorption spectrum which did not show any signs of splitting of the α, β, or Soret bands.

As the sulfonato groups are separated from the cavity of the porpyrin macrocycle by the *ortho*-methyl substituents on the *meso*-phenyl rings, they should not influence a metal ion chelated to the pyrrole nitrogen atoms. Electronic effects should be the same since all sulfonato substituents are in meta positions. As shown by spectrophotometric titration (vide infra), the central iron(III) of the synthesized mixture of atropisomers 3-Fe^{III} must be electronically much the same. The only complication one has to be concerned about is the effect of the anionic sulfonato groups in the different atropisomers on the overall polarity of the molecule.

Synthesis of Iron(III) [5,10,15,20-Tetrakis(2,6-dimethyl-3-sulfonatophenyl)porphyrin] (3-Fe^{III}). 3 was metalated by refluxing with a large excess of ferrous sulfate in water between pH 5.0 and 8.0. After extensive purification the product displayed two spots on a reversed-phase thin-layer chromatogram in a ratio of relative areas of approximately 2:1. The product could be resolved by HPLC to two peaks with relative areas of 65 and 35%, respectively. This indicates again the presence of more than one atropisomer. These are likely to be the most prevalent ones ("three up, one down" and cis "two up, two down") plus possibly one minor atropisomer. Elemental analysis for the product could be accommodated to a molecular composition of $[3\text{-}Fe^{III}Na_4]^+(SO_4^{2-})_{0.5} \times 16H_2O$.

The electronic absorption spectrum (Figure 1) of 3-Fe^{III} at pH 3.25 compares well with that reported for the iron(III) [tetrakis(4-sulfonatophenyl)porphyrin] diaquo complex (4-Fe^{III}-$Na_3(H_2O)_2$).[11c] The spectrum taken in basic solution (pH 9.71), however, showed no similarity in its α,β-region to the spectrum of the μ-oxo dimer of 4-Fe^{III}.[11c] This is reasonable, since 3-$Fe^{III}(OH)$ is not expected to form a μ-oxo dimer due to steric hindrance by its eight *ortho*-methyl groups. On the other hand, the spectrum reveals considerable similarity with that reported for 4-$Fe^{III}(OH)$, observed by rapid scanning techniques in stopped-flow experiments.[17]

The structural assignment was further substantiated by ^1H NMR spectroscopy. In D_2O with a trace of DCl added, the β-pyrrole-H resonance for 3-$Fe^{III}(H_2O)_2$ was found at δ 45.5 (half-width $\sim$ 180 Hz; 8 H). Such a pronounced upfield shift of the β-pyrrole-H resonance, as compared to δ 80 diagnostic for

(17) El-Awady, A. A.; Wilkins, P. C.; Wilkins, R. G. *Inorg. Chem.* **1985**, *24*, 2053.

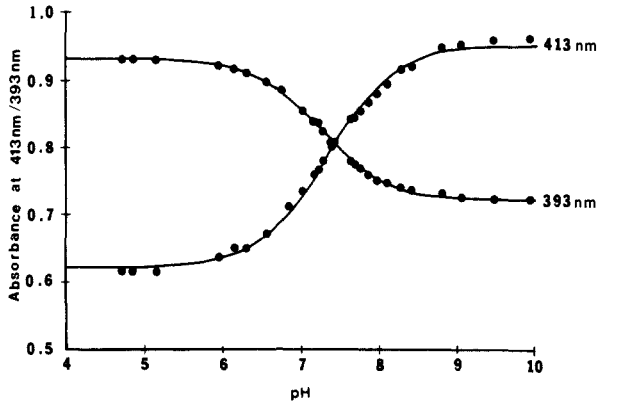

Figure 2. Spectrophotometric titration to determine the pK_a of water ligated to 3-Fe^{III} (30 °C, [3-Fe^{III}] = 3.09 × 10^{-6} M, d = 3.387 cm, solvent water).

a "normal" high-spin iron(III) porphyrin,[18] has been taken as an indication for the presence of an "admixed intermediate" ($S = {}^3/_2, S = {}^5/_2$) spin state of iron(III) porphyrin complexes.[19-21] It is known, however, that diaquo(*meso*-tetraphenylporphinato)-iron(III) perchlorate contains a hexacoordinated, high-spin ($S = {}^5/_2$) central atom.[21,22] The observed difference could be due to the fact that water in aqueous solution is presumably acting as a weaker ligand than when it is present as an isolated molecule in an unpolar organic solvent. This could cause a smaller crystal-field splitting for the complex 3-$Fe^{III}(H_2O)_2$.

Two singlets integrating for 4 H each at δ 10.50 and 9.37 for the protons in the meta and para positions of the phenyl rings and two multiplets between δ 4.0 and 2.0 integrating for 24 H, for the *ortho*-methyl substituents, are assigned in analogy to literature data.[13,18,19] The appearance of merely a broad singlet for the meta protons can be taken as another sign for the hexacoordination and consequent planarity of 3-$Fe^{III}(H_2O)_2$. The spectrum of 3-Fe^{III} in D_2O/NaOD features much broader and less resolved resonances, which are difficult to assign to specific positions of the molecule: δ 80 (br s, half-width 1500 Hz), 14–13, 13–12 (2 m), 9.5–8.5 (2 m), 3.7–2.0 (several m). A broadening of line widths for hydroxy-ligated iron–porphyrins has been reported.[19] The broad β-pyrrole-H resonance at δ 80 is a hint to the presence of the 3-Fe^{III}OH species. The ^1H NMR cannot be taken as proof, however, for the complete absence of any μ-oxo dimer of 3-Fe^{III}.[13] On the basis of these results and on the analogy to the established fact that iron(III) tetramesitylporphyrin hydroxide (5-Fe^{III}OH) does not form a μ-oxo dimer in organic solvent,[13] it is reasonable to assume that 3-Fe^{III} is also present in aqueous solution at higher pH as an hydroxy-ligated species.

The absence of molecular association of 3-Fe^{III} in water was verified by showing that its absorbance as a function of concentration (1.0×10^{-3}–1.3×10^{-6} M) follows Beer's law at pH 3.25 (657 nm, 528 nm), 4.96 (393 nm), and 9.71 (413 nm). On going from ionic strength 0 to 1.9 with potassium chloride there was no distinct alteration of the Soret band (pH 4.96); merely an 8% drop in the maximum absorption was observed, which could be explained by a change in solvent polarity. This also demonstrates that there is no ligation by chloride under these conditions.

The possibility of demetalation of 3-Fe^{III} under acidic conditions was examined. A sample of the ferric porphyrin, dissolved in 1 N hydrochloric acid, showed a 3% decrease of the maximum absorption of the Soret band after 24 h at 30 °C; this is within acceptable error. No other new peaks could be detected in the spectrum. This indicates that 3-Fe^{III} exhibits exceptional stability

(18) (a) LaMar, G. N.; Eaton, G. R.; Holm, R. H.; Walker, F. A. *J. Am. Chem. Soc.* **1973**, *95*, 63. (b) LaMar, G. N. ; Walker, F. A. In *The Porphyrins*; Dolphin, D., Ed.; Academic Press: New York, 1979; Vol. IVB, p 61.
(19) Goff, H.; Shimonura, E. *J. Am. Chem. Soc.* **1980**, *102*, 31.
(20) Reed, C. A.; Mashiko, T.; Bentley, S. P.; Kastner, M. E.; Scheidt, W. R.; Spartalian, K.; Lang, G. *J. Am. Chem. Soc.* **1979**, *101*, 2948.
(21) Scheidt, W. R.; Reed, C. A. *Chem. Rev.* **1981**, 543.
(22) Scheidt, W. R.; Cohen, I. A.; Kastner, M. E. *Biochemistry* **1979**, *18*, 3546.

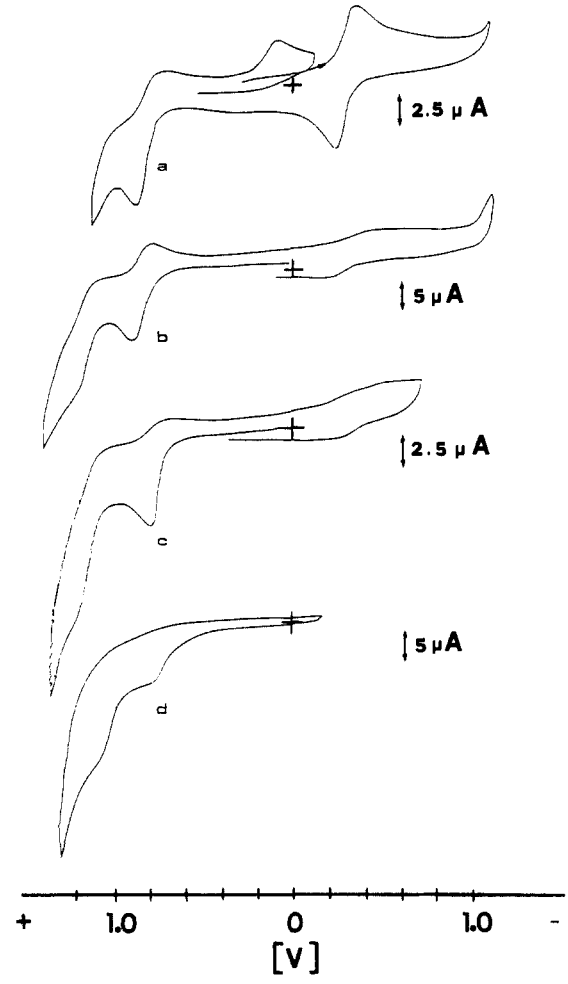

Figure 3. Cyclovoltammograms (CV) with glassy carbon electrode of water-soluble iron(III) porphyrins 3-Fe^{III} and 4-Fe^{III} at different pH values (100 mV/s). (a) CV of 4-Fe^{III}, c = 1.38 mM, 0.08 M KH-phthalate buffer, pH 3.25, scan. (b) CV of 3-Fe^{III}, c = 1.20 mM, 0.10 M KH-phthalate, pH 4.97. (c) CV of 3-Fe^{III}, c = 0.60 mM, 0.10 M KH_2PO_4, pH 7.00 (d) CV of 3-Fe^{III}, c = 0.6 mM, 0.05 M Na_2HPO_4, pH 11.10.

toward acids. To our knowledge this has been the first investigation that has covered this low pH range in a porphyrin model study.

Determination of the pK_a of Water Ligated to 3-Fe^{III}. The pK_a of water ligated to 3-Fe^{III} was determined by spectrophotometric titration at 393 and 413 nm (Figure 2) and was found to be 7.25

$$3\text{-}Fe^{III}(H_2O)_2 \overset{K_a}{\rightleftharpoons} 3\text{-}Fe^{III}(H_2O)(OH) + H^+ \qquad (1)$$

± 0.05. The value obtained at five different wavelengths (393, 413, 480, 528, 600 nm) in three different titration experiments was 7.24 ± 0.08. This shows that the two or three atropisomers present possess indistinguishable pK_a values. This finding provides valuable evidence that the electronic influence of the iron(III) ion on its axial ligands is quite the same for the different atropisomers of 3-Fe^{III}. A second deprotonation step could not be observed spectrophotometrically on increasing the pH to 14. The pK_a of water is lowered by ligation to the central metal ion by approximately 7 units. This is of interest for the reaction of iron(III) porphyrins with hydroperoxides where the lowering of the acid dissociation constant of the hydroperoxide on its ligation to the metalloporphyrin must be of importance to the mechanism and facility of the reaction.

Electrochemistry of 3-Fe^{III}. Cyclovoltammetric experiments with 3-Fe^{III} and 4-Fe^{III} were conducted in aqueous buffer solutions (25 °C) at different pH values (Figure 3). Freshly polished glassy carbon was utilized as the working electrode. The metalloporphyrin adsorbs readily to the electrode surface so that after about five scans the shape and position of the electrochemical waves change considerably. The most notable feature of the cyclic voltammograms is that 3-$Fe^{III}(H_2O)_2$ shows a nicely reversible oxidation wave at 860 mV. This is in contrast to 4-$Fe^{III}(H_2O)_2$ which exhibits a first oxidation at 820 mV, which is only partly reversible. At 180 mV one additionally observes the reduction of a compound formed by chemical reaction of the $1e^-$ oxidation product of 4-$Fe^{III}(H_2O)_2$. This reductive wave is probably attributable to an iron(III) isoporphyrin formed by addition of a nucleophile (water, OH^-) to the meso position of the porphyrin π-cation radical generated in the first oxidation step. Such a nucleophilic attack cannot occur upon the π-cation radical of the hydrate of the iron(III) complex of 3 ($^{\bullet+}$3-$Fe^{III}(H_2O)_2$), where the meso positions of the porphyrin ring are sterically protected by the *ortho*-methyl substituents of the *meso*-phenyl rings.

When the pH is raised, the potential of the first oxidation becomes less positive and its reversibility decreases (pH 7.00, $E_{1/2}$ = 750 mV, cathodic peak current/anodic peak current = 0.25) and, finally (pH 11.10), only shows up as a shoulder around 700 mV in the next (irreversible) oxidative wave at 1010 mV. A plausible explanation for this behavior is that with 3-$Fe^{III}(H_2O)_2$ the first oxidation leads to an iron(III) porphyrin π-cation radical, while in the case of the hydroxy-ligated ferric porphyrin the central metal atom itself is oxidized to an iron(IV)-oxo species. The iron(IV)-oxo species is proposed to react further by oxidizing water or the porphyrin.[12e,23] From our physical characterization of 3-Fe^{III} we conclude that it is a reasonably well-behaved water-soluble porphyrin, suitable for the investigation of oxidative metalloporphyrin model chemistry in aqueous systems.

Kinetics of the Reaction of 3-Fe^{III} with Hydrogen Peroxide. It is known that iron(III) porphyrins are degraded by excess hydrogen peroxide in the absence of an oxidizable substrate. This is also the case with 3-Fe^{III}, which is evident from the rapid decay of the Soret band after addition of excess hydrogen peroxide to a solution of 3-Fe^{III}. As was shown by Portsmouth and Beal[5f] and Traylor, Lee, and Stynes,[5m] decomposition of the porphyrin can be prevented by adding a readily oxidized compound, which in a rapid step traps the generated higher valent iron-oxo species, thus keeping it from attacking and destroying the porphyrin (cf. Scheme I; AH = trapping species). At the same time, by following the formation of the oxidized trapping agent one can obtain rate constants for the rate-determining step of formation of the higher valent iron-oxo species. In the net reaction the iron(III) porphyrin acts as a catalyst to oxidize a substrate by H_2O_2.

As a water-soluble trap we chose 2,2'-azinobis(3-ethylbenzthiazoline)sulfonic acid(6) (ABTS),[24] a compound recently introduced for clinical peroxidase assays because of its superb characteristics.[25] ABTS on oxidation forms a stable green cation radical ($ABTS^{\bullet+}$) with several strong absorptions in the visible and near infrared. The formation of $ABTS^{\bullet+}$ is conveniently followed at its λ_{max} at 660 nm (ϵ = 12000 M^{-1} cm^{-1}).[24] The oxidation potential of ABTS as well as the comproportionation constant for the $2e^-$ oxidized and the fully reduced species to

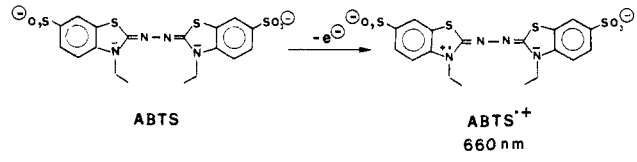

provide $ABTS^{\bullet+}$ is invariable over a wide range of pH.[24] The combination of reagents 3-Fe^{III}, ABTS, and hydrogen peroxide was first evaluated in 100 mM acetate buffer at pH 5.20 (μ = 0.20 with sodium nitrate). It was shown, by observation of the

(23) Cf.: Arena, F.; Gans, P.; Marchon, J.-C. *J. Chem. Soc., Chem. Commun.* **1984**, 196.

(24) Huenig, S.; Balli, H.; Conrad, H.; Schott, A. *Justus Liebigs Ann. Chem.* **1964**, *676*, 32, 36, 52.

(25) (a) Gawehn, K.; Wielinger, H.; Werner, W. *Z. Anal. Chem.* **1970**, *252*, 222. (b) Werner, W.; Rey, H.-G.; Wielinger, H. *Z. Anal. Chem.* **1970**, *252*, 224. (c) Gallati, H. *J. Clin. Biochem.* **1979**, *17*, 1. (d) Puetter, J.; Becker, R. In *Methods of Enzymatic Analysis*, 3rd ed.; Bergmeyer, H. U., Ed.; Verlag Chemie: Weinheim, 1983; Vol. 3, p 286.

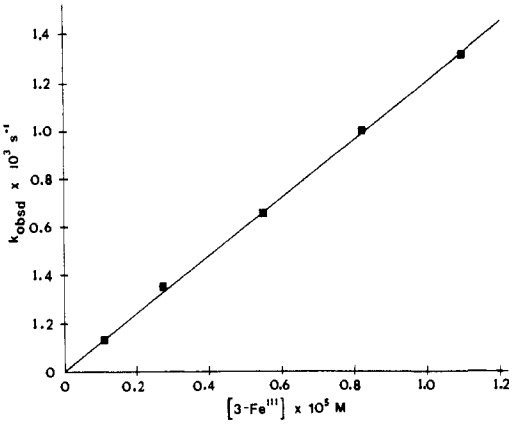

Figure 4. Observed first-order rate constants for $ABTS^{\bullet+}$ formation as a function of [3-Fe^{III}] in 50 mM acetate buffer, pH 5.20 (μ = 0.20 with $NaNO_3$) at 30 °C. $[H_2O_2]$ = 1.25 × 10^{-4} M; [ABTS] = 7.6 × 10^{-3} M.

Soret band, that acetate binds to 3-Fe^{III} with an equilibrium constant of approximately 1 M^{-1}. In the absence of iron(III) porphyrin a solution of ABTS and H_2O_2 is stable for several hours without showing any formation of $ABTS^{\bullet+}$. Addition of 3-Fe^{III} leads to an immediate appearance of $ABTS^{\bullet+}$. For kinetic studies, the substrate H_2O_2 was used in a minimal tenfold excess over 3-Fe^{III} catalyst which usually was maintained at 5 × 10^{-6} to 1 × 10^{-7} M. In practice, a 50- to 70-fold excess of ABTS over hydrogen peroxide was employed. Under these conditions the formation of $ABTS^{\bullet+}$ followed the first-order rate law. The observed rate constants (k_{obsd}) were independent of [ABTS]. Both ABTS and its immediate oxidation product $ABTS^{\bullet+}$ were stable under the experimental conditions and within the time frame of the experiment.

By fitting the plots of $ABTS^{\bullet+}$ appearance (ΔA_{660}) vs. time to the first-order rate law there were obtained the pseudo-first-order rate constants (k_{obsd}), under turnover conditions, for the formation of the intermediate higher valent porphyrin iron–oxo species. Values of k_{obsd} were found to be independent of the initial concentration of hydrogen peroxide ($[H_2O_2]_i$). Analysis of plots of A_{660} vs. time at varying $[H_2O_2]_i$ by the method of initial rates provided rates for the appearance of $ABTS^{\bullet+}$. A plot of these initial rates vs. $[H_2O_2]_i$ was linear with slope (at [3-Fe^{III}] = 1.46 × 10^{-6} M, [ABTS] = 5.0 × 10^{-3} M) equal to 2.70 × 10^{-4} s^{-1}. This linearity demonstrates that the reaction is truly first order in $[H_2O_2]$ and that the catalyst is not saturated in this species. The final absorbance at 660 nm was directly proportional to $[H_2O_2]_i$, and a plot of the absorbance at infinity vs. $[H_2O_2]_i$ had zero intercept and a slope of 16 300 M^{-1} cm^{-1}, corresponding to a 68 % yield of $ABTS^{\bullet+}$. From this finding and from the fact that the velocity of formation of $ABTS^{\bullet+}$ should be twice that of the disappearance of H_2O_2 (assuming a 2:1 stoichiometry: $d[ABTS]/dt = -2d[H_2O_2]/dt$), the value of the first-order rate constant of H_2O_2 disappearance can be calculated as 1.99 × 10^{-4} s^{-1}. This can be compared with the average value of k_{obsd} = 2.07 × 10^{-4} s^{-1} obtained by first-order methods from the plots of the appearance of $ABTS^{\bullet+}$ with time. The reader is reminded that, though the formation of 2$ABTS^{\bullet+}$ per H_2O_2 reacting need not be taken into account when following the reaction to completion and fitting its course to the first-order rate law, the formation must be taken into account when the method of initial rates is used. In Figure 4 there is shown a plot of the observed pseudo-first-order rate constant (k_{obsd}) for formation of $ABTS^{\bullet+}$ vs. concentration of 3-Fe^{III}, demonstrating the first-order dependence of k_{obsd} upon the ferric porphyrin concentration. No deviation from a linear relationship, which was commonly observed in earlier investigations and attributed to aggregation and dimerization of the catalyst,[5a-i] is seen in the graph. Thus, the formation of $ABTS^{\bullet+}$ follows the rate law of eq 2a and the rate-determining step involves reaction

$$-d[H_2O_2]/dt = k_2[\text{3-Fe}^{III}][H_2O_2] \quad (2a)$$

$$k_{obsd} = k_2[\text{3-Fe}^{III}] \quad (2b)$$

Table I. Buffer-Catalyzed (k_{BT}) and Lyate (k_{ly}) Rate Constants for the Reaction of 3-Fe^{III} with Hydrogen Peroxide in Different Buffers at Several pH Values

pH	buffer	k_{BT} [M^{-2} s^{-1}]	k_{ly} [M^{-1} s^{-1}]	k_{BT}/k_{ly} [M^{-1}]
2.73	chloroacetate	146	39	3.7
3.95	acetate	74	54	1.4
5.20	acetate	267	93	2.9
6.18	collidine	1.69 × 10^4	343	49
6.98	collidine	3.75 × 10^4	957	39
7.77	collidine	5.85 × 10^4	1580	37
8.00	phosphate	−8.61 × 10^3	2150	−4.0
8.64	collidine	7.51 × 10^4	2820	27
9.28	carbonate	0	4840	0
9.85	carbonate	−5.82 × 10^4	1.55 × 10^4	−3.8

of hydrogen peroxide with iron porphyrin. The second-order rate constant k_2 can be calculated as:

$$k_2 = k_{obsd}/[\text{3-Fe}^{III}] \quad (2c)$$

Effect of Buffers on the Rate of Reaction of 3-Fe^{III} with H_2O_2. The second-order rate constants k_2 for the reaction of 3-Fe^{III} (at 4 × 10^{-6} to 4 × 10^{-7} M) with H_2O_2 were determined at given pH values with four different concentrations of buffer at each pH. In these experiments the pH of the buffer solutions was adjusted to within 0.02 pH unit of the desired values. Reactions which showed more than 0.03 deviation in pH at completion were discarded. The slopes of the plots of total buffer concentration ([BT]) vs. k_2 provide the pH-dependent constants k_{BT} and the intercept the pH-dependent second-order rate constants for the lyate rate (k_{ly}) as shown in eq 3. The following buffers and concentrations

$$k_2 = k_{BT}[BT] + k_{ly} \quad (3)$$

were used: $ClCH_2COOH/ClCH_2COO^-$ (pH 2.73, [BT] = 8 × 10^{-3}–8 × 10^{-2} M), CH_3COOH/CH_3COO^- (pH 3.95 and 5.20, [BT] = 1 × 10^{-2}–1 × 10^{-1} M), 2,4,6-collidine·HCl/2,4,6-collidine (pH 6.18 to 8.64, [BT] = 4 × 10^{-3}–6 × 10^{-2} M), $H_2PO_4^-/HPO_4^{2-}$ (pH 8.00, [BT] = 2 × 10^{-3}–5 × 10^{-2} M), HCO_3^-/CO_3^{2-} (pH 9.28 and 9.85, [BT] = 8 × 10^{-3}–8 × 10^{-2} M). Determined values of k_{BT} and k_{BT}/k_{ly} are shown in Table I. Inspection of Table I shows that carbonate and phosphate buffers exhibit either no effect or a slightly inhibiting effect on rate while acetate/acetic acid and chloroacetate/chloroacetic acid buffers, at given pH, exhibit a very minor rate accelerating effect. Since acetate buffer shows no catalysis at pH 3.95 and the reaction is $[H_3O^+]$ insensitive at low pH, the chloroacetate buffer effect is most likely other than general catalysis. The small increase in rate with acetate buffer at pH 5.20 may be associated with acetate general base catalysis. Collidine/collidine·H^+ is the only buffer system which shows a credible catalytic effect. Shown in Figure 5 are plots of k_{obsd} vs. [3-Fe^{III}] at different concentrations of collidine buffer at pH 6.98. The apparent second-order rate constants (k_2) at several pH values, derived from graphs similar to Figure 5, are represented vs. the total collidine buffer concentration in Figure 6. If the reaction was only catalyzed by collidine and not by protonated collidine then plots of k_2 vs. collidine free base concentrations (plots not shown) at various pH values should be parallel since the slopes would equal the rate constant (k_B) for collidine free base catalysis. However, plots of k_2 vs. the concentration of free collidine base were not parallel. These results suggest the importance of catalysis by both buffer species. If this is so then it is to be expected[26] that a plot of k_{BT} vs. [collidine free base]/[total collidine] will yield a straight line with non-zero intercept. Such a plot is shown in Figure 7. From the intercepts at [collidine]/([collidine] + [collidine·H^+]) = 0 and 1, respectively, the rate constants for catalysis by protonated collidine (k_{BH^+} = 2.0 × 10^4 M^{-2} s^{-1}) and collidine free base (k_B = 8.2 × 10^4 M^{-2} s^{-1}) can be obtained.

The Dependence of k_{ly} upon pH for the Reaction of 3-Fe^{III} with H_2O_2. In order to obtain values of k_{ly} outside of the pH range employed in the study of buffer catalysis, rate constants were

(26) Jencks, W. P. *Catalysis in Chemistry and Enzymology*; McGraw-Hill: New York, 1969; p 166.

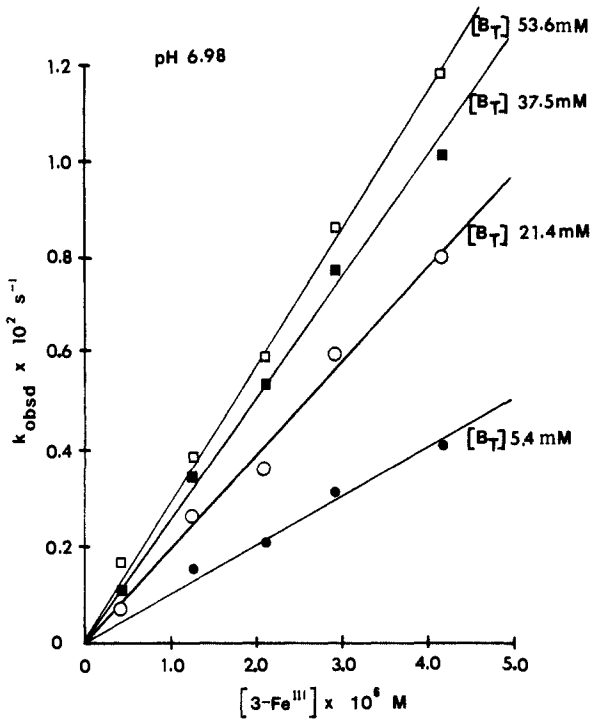

Figure 5. Dependence of the pseudo-first-order rate constants (k_{obsd}) for the formation of the peroxidatic intermediate of 3-Fe^{III} on the concentration of collidine buffer at pH 6.98. $[H_2O_2] = 4.50 \times 10^{-5}$ M; [ABTS] = 3.37×10^{-3} M.

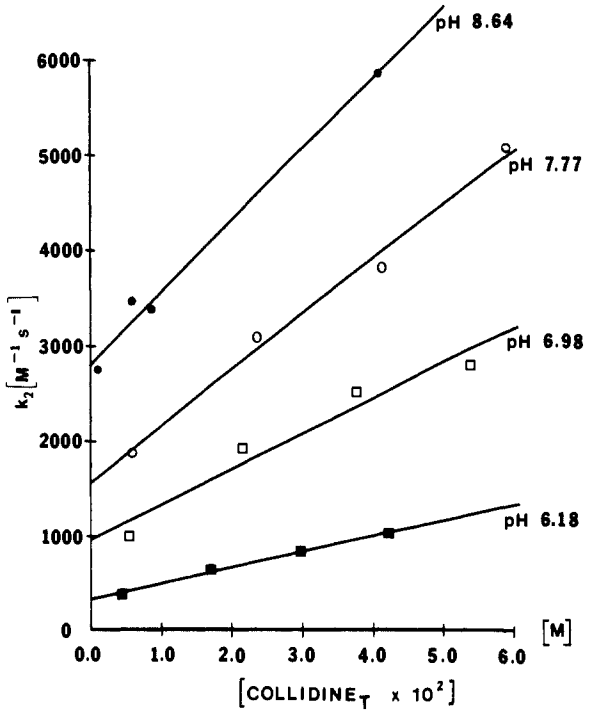

Figure 6. Change in second-order rate constants (k_2) with change in the concentration of total collidine at different pH values. Every k_2 value is derived from a plot of k_{obsd} vs. [3-Fe^{III}] (cf. Figure 5).

determined at pH 0.99 (hydrochloric acid) and pH 11.06 and 12.00 (sodium hydroxide). In these pH regions the buffer capacities of $[H_3O^+]/[H_2O]$ and $[H_2O]/[HO^-]$ are sufficient to maintain constant pH. Below pH 4, there was found to be a slow zero-order formation of ABTS$^{\cdot+}$ superimposed on the more rapid pseudo-first-order reaction. The time course of the experiments could be fitted by employing a computer program for simultaneous zero- and first-order formation of product. By this means the rate constants for the zero-order and first-order processes (k_{obsd}) were obtained. By performing the kinetic runs anaerobically, it was

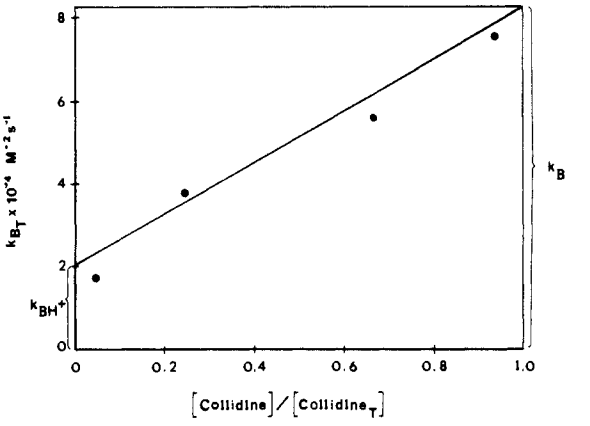

Figure 7. Variation of k_{BT} with the mole fraction of free collidine. The intercept at X (free collidine) = 0 gives k_{BH^+}, and the intercept at X (free collidine) = 1 gives k_B.

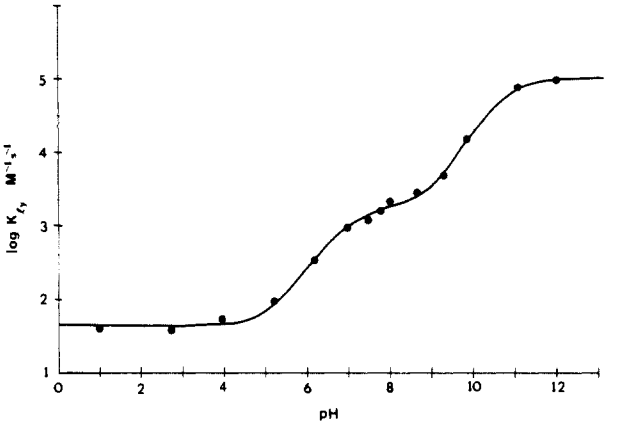

Figure 8. Plot of the log of the rate constants for nonbuffer catalyzed (k_{ly}) reaction of 3-Fe^{III} with hydrogen peroxide vs. pH (30 °C, μ = 0.20 M).

Table II. Values of Rate and Equilibrium Constants Obtained from the Fitting of Equation 4 to the Experimental Points of Figure 8

k_a	44		
k_b	1.67×10^3		
k_c	1.05×10^5		
K_A	1.55×10^{-7}	pK_A	6.8
K_B	2.03×10^{-11}	pK_B	10.7

shown that the zero-order reaction is oxygen dependent while the first-order rate constant is not. The zero-order rate constants show a linear dependence on [3-Fe^{III}] and pertain to a reaction of 3-Fe^{III}, O_2, and ABTS. Though interesting, this reaction is not of concern to the present study. In the presence of O_2 and absence of 3-Fe^{III}, ABTS is stable at acid pH values. At these low pH values the reaction of the 3-Fe^{III} with H_2O_2 is so slow that decomposition of hydrogen peroxide by adventitiously present impurities is noticeable and non-zero intercepts are obtained in the plots of k_{obsd} vs. [3-Fe^{III}]. However, the slopes of these plots are all that was sought since they equal the desired second-order rate constants (k_2) for the porphyrin-catalyzed reaction. At pH values >10, ABTS$^{\cdot+}$ is not stable indefinitely under the experimental conditions. Good first-order fits for the experimental data were, nevertheless, obtained for at least 6 half-lives.

The pH dependence of the buffer-independent second-order lyate rate constants (k_{ly}, eq 3) is best appreciated by examination of a plot of log k_{ly} vs. pH as shown in Figure 8. The points of Figure 8 are experimental, and the line which fits (with a standard error of 4.74×10^{-2}) these points has been generated by computer iteration with use of the empirical eq 4. The values for the derived

$$k_{ly} = \frac{k_a a_H}{(K_a + a_H)} + \frac{k_b K_A}{(K_a + a_H)} + \frac{k_c K_A K_B}{(K_a + a_H)(K_a + a_H)} \quad (4)$$

constants are given in Table II. Inspection of Figure 8 shows

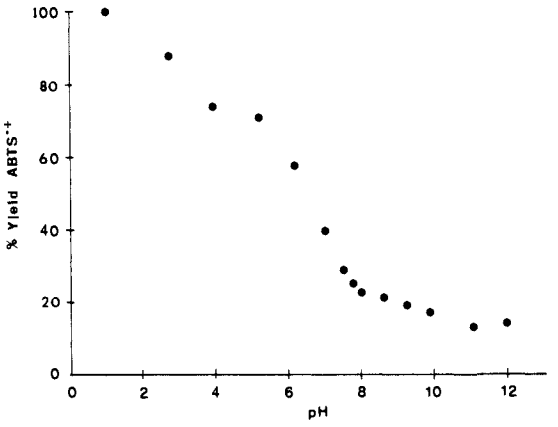

Figure 9. Variation of the yield of $ABTS^{\cdot+}$ (for ten turnovers of the catalyst 3-Fe^{III}) with the pH of the reaction medium. The percentage yields of $ABTS^{\cdot+}$ are calculated on the basis that consumption of one H_2O_2 provides two $ABTS^{\cdot+}$.

the presence of three pH-independent plateaus at low, intermediate, and high pH and two inflections in the intermediate regions.

Effect of the Change in the Composition of the Solvent on the Rate of Reaction. A series of experiments was conducted at pH 8.48 (collidine buffer) in water containing 14.5% methanol (v/v, μ = 0.20 with $NaNO_3$, 30 °C) under the same conditions as employed in water. The rate constants for lyate and buffer species catalysis were determined as k_{ly} = 1250 M^{-1} s^{-1} and k_{BT} = 2.17 × 10^4 M^{-2} s^{-1} (k_{BT}/k_{ly} = 17 M^{-1}). The effect of ionic strength on the rate of the reaction was examined by the determination of a single value of k_2 (eq 2c) at pH 8.64 and μ = 0.05 ([collidine$_T$] = 0.04 M) in water. The value of k_2 of 5330 M^{-1} s^{-1} may be compared to that at μ = 0.2 of 5820 M^{-1} s^{-1}.

Dependence of Yields of $ABTS^{\cdot+}$ on Experimental Conditions. There was no significant alteration in the yield of $ABTS^{\cdot+}$ with variation of buffer concentrations at constant pH. Most conspicuous is the dependence of the yields on the pH. For 10 turnovers of catalyst, formation of $ABTS^{\cdot+}$ occurred to 100% at pH 1 and only ~20% at pH 12 (percentage yields based upon two $ABTS^{\cdot+}$ per one H_2O_2 reacted). The plot of percent yield of $ABTS^{\cdot+}$ vs. pH shows a sharp drop between pH 5 and 9 with an inflection around pH 7 (Figure 9). By employing an oxygen electrode in a sealed reaction chamber without an air space, it was shown that oxygen evolution occurs in the reaction. This oxygen most likely originates from a disproportionation of H_2O_2 catalyzed by 3-Fe^{III}. In this reaction H_2O_2 apparently competes as substrate with ABTS for the higher valent iron–oxo porphyrin which is formed in the rate-determining reaction of one molecule of H_2O_2 with 3-Fe^{III}. Thus, lower yields of $ABTS^{\cdot+}$ should go parallel with higher ratios of O_2 formation. At the same time, the rate constants for O_2 and $ABTS^{\cdot+}$ formation should be the same for a given set of experimental conditions. That this was true was shown by the following experiments: Rate constants for O_2 evolution were determined by fitting the experimental plots of percent saturation of O_2 in water vs. time to the first-order rate law. Second-order rate constants were calculated with eq 2c. In phosphate buffer at pH 8.00 ([3-Fe^{III}] = 1.7 × 10^{-6}–2.4 × 10^{-6} M, [H_2O_2] = 3.5 × 10^{-4} M, [ABTS] = 12.35 × 10^{-3} M, [B_T] = 0.04 M, μ = 0.2, 30 °C) the second-order rate constant for oxygen formation was k_2 = 1640 ± 160 M^{-1} s^{-1}, which can be compared with k_2 = 1810 M^{-1} s^{-1} for $ABTS^{\cdot+}$ formation at the identical pH (calculated with eq 3; [3-Fe^{III}] = 4 × 10^{-7}–4 × 10^{-6} M, [H_2O_2] = 4.5 × 10^{-5} M, [ABTS] = 3.4 × 10^{-3} M, [B_T] = 0.04 M, μ = 0.2, 30 °C). In acetate buffer at pH 5.20 ([3-Fe^{III}] = 3.25 × 10^{-6} M, [H_2O_2] = 4.3 × 10^{-4} M, [ABTS] = 12.2 × 10^{-3} M, [B_T] = 0.07 M, μ = 0.2, 30 °C) the second-order rate constant for O_2 formation was 110 M^{-1} s^{-1} which can be compared to k_2 = 112 M^{-1} s^{-1} for $ABTS^{\cdot+}$ formation at the same pH ([3-Fe^{III}] = 4.5 × 10^{-7}–4.5 × 10^{-6} M, [H_2O_2] = 4.5 × 10^{-4} M, [ABTS] = 3.4 × 10^{-3} M, [B_T] = 0.07 M, μ = 0.2, 30 °C). The amount of oxygen evolved at pH 5.20 was approximately half of that produced at pH 8.00. This is in agreement with the observed yields of $ABTS^{\cdot+}$, which are twice as large at pH 5.20 as at pH 8.00.

The relative yields of $ABTS^{\cdot+}$ decreased with the number of turnovers of catalyst. The yield of $ABTS^{\cdot+}$ produced by 100 turnovers of catalyst was 70 to 85% of the yield obtained for 10 turnovers of 3-Fe^{III}.

Discussion

The reaction of hydrogen peroxide with a ferric porphyrin in aqueous medium has been reinvestigated.[5] For this purpose we utilized the novel iron(III) 5,10,15,20-tetrakis(2,6-dimethyl-3-sulfonatophenyl)porphyrin (abbreviated as 3-Fe^{III}). 3-Fe^{III} is water soluble but does not aggregate nor does it form a μ-oxo dimer. Due to the particular substitution pattern of its phenyl rings 3-Fe^{III} consists as a mixture of four atropisomers. All discussion of this topic is provided in the Results. An isomer mixture of only approximately known composition was employed in our studies. Because the sulfonato groups are well separated from the central metal atom of 3-Fe^{III}, it was not expected that the occurrence of atropisomerism would cause any complications in reactions involving the ligated iron(III). Support for this expectation is found in the observation that the changes in absorbance of 3-$Fe^{III}(H_2O)_2$ for the atropisomer mixture which accompany change of pH fit well to a theoretical titration curve for a single monobasic acid (Figure 2). From Figure 2, one of the water molecules present as an axial ligand in 3-$Fe^{III}(H_2O)_2$ undergoes proton dissociation with pK_a 7.25 to form 3-$Fe^{III}(H_2O)(OH)$. The $1e^-$ oxidized species derived from 3-$Fe^{III}(H_2O)_2$ is stable within the time frame of CV experiments (scan speed 100 mV/s, water solvent), while the $1e^-$ oxidized form of 3-$Fe^{III}(H_2O)(OH)$ as well as the $2e^-$ oxidized forms undergo further reactions under the conditions of the CV experiments.

The kinetics of oxygen transfer from H_2O_2 and HOO^- to the aquo species of 3-Fe^{III} as a function of pH and buffer concentration were studied in aqueous solution at constant and known pH values at 30 °C and μ = 0.2 with $NaNO_3$. In the reactions of 3-Fe^{III} with hydrogen peroxide, degradation of the porphyrin could be prevented by utilizing the easily oxidizable substrate, ABTS, as a trap to reduce the generated higher valent iron–oxo complex. In the trapping reaction, each H_2O_2 consumed results in the competitive oxidation of two ABTS molecules to yield two $ABTS^{\cdot+}$ species or in the oxidation of a hydroperoxide species. Formation of $ABTS^{\cdot+}$ was followed spectrophotometrically (660 nm) with time as a means of monitoring the time course of the reaction. The reaction was found to be first order in 3-Fe^{III}, first order in hydrogen peroxide, and zero order in ABTS (eq 2a). The apparent second-order rate constants for reactions of 3-Fe^{III} with H_2O_2 (k_2) are composed of terms for buffer catalysis (k_{BT}) and lyate catalysis (k_{ly}) (eq 3).

Increase of hydroxide ion concentration by 10^{11} increases the value of k_{ly} by only $10^{2.5}$. Thus, the reaction of hydrogen peroxide with iron(III) porphyrin is not simply first order in [HO^-] as previously claimed.[5e,i,k,l] This is also evident from the pH–rate profile (Figure 8). Equation 4 provides the mathematical fit of the log k_{ly} vs. pH data of Figure 8. Inspection of eq 4 shows that three different mechanisms for decomposition of hydrogen peroxide by the iron(III) porphyrin are operative between pH 1 and 12. The stoichiometry of the three transition states differs in the number of protons involved. The three reaction paths are related to one another by the acid–base dissociation constants K_A and K_B. The simplest sequence of reactions, in agreement with these data, is depicted in Scheme II. At low pH the reacting species are the iron(III) porphyrin bis-aquo complex I and H_2O_2; at intermediate pH the hydroxy-ligated iron(III) porphyrin complex III and H_2O_2; and at high pH, complex III and the hydroperoxy anion. A preequilibrium treatment of Scheme II yields eq 5a for the second-order rate constant k_{ly}.

$$k_{ly} = \frac{k_1'K_1a_H^2 + k_2'K_2K_aa_H + k_3'K_3K_aK_H}{K_HK_a + (K_H + K_a)a_H + a_H^2} \qquad (5a)$$

At low pH, $a_H \sim K_a \gg K_H$ and

$$k_{ly} = k_1'K_1a_H/(K_a + a_H) = k_{(A)} \qquad (5b)$$

At intermediate pH, $K_a > a_H > K_H$ and

$$k_{ly} = k_2'K_2K_a/(K_a + a_H) = k_{(B)} \quad (5c)$$

At high pH, $K_a \gg K_H \sim a_H$ and

$$k_{ly} = k_3'K_3K_aK_H/(K_a + a_H)(K_H + a_H) = k_{(C)} \quad (5d)$$

An appropriate equation (eq 6) to fit the log k_{ly} vs. pH profile is obtained by summation of eq 5b,c,d.

$$k_{ly} = k_{(A)} + k_{(B)} + k_{(C)} \quad (6)$$

Comparison of eq 6 with the experimentally derived, empirical eq 4 gives

$$k_a = k_1'K_1;\ k_b = k_2'K_2;\ k_c = k_3'K_3$$

$$K_A = K_a;\ K_B = K_H$$

The values of k_a, k_b, k_c, K_A, and K_B are obtained from the mathematical fit of the log k_{ly} vs. pH profile (Figure 8) and are given in Table II. It should be noted that the second-order rate constants k_a, k_b, and k_c are products of equilibrium constants (K_1, K_2, and K_3) for association of iron(III) porphyrin and hydrogen peroxide species and rate constants (k_1', k_2', and k_3') for oxygen transfer to the iron(III) of the porphyrin. The values of K_1, K_2, and K_3 are unknown so that the values of k_1', k_2', and k_3' for oxygen transfer may not be computed. The equilibrium constants K_1 and K_2 involve the ligation of H_2O_2 to ferric porphyrin species where, in the first instance, the central iron(III) holds a formal positive charge and, in the second instance, is neutral. It follows, therefore, that $K_1 > K_2$. Complexes of iron(III) porphyrins possessing two negatively charged anions (CN^-, HO^-, etc.) as axial ligands are unknown. Since K_3 involves the ligation of HOO^- to a porphyrin species where the central iron(III) is already ligated to HO^- it follows that $K_1 > K_2 > K_3$. Thus, the increase of k_{ly} on raising the pH (i.e., going from the first to the second to the third plateau of Figure 8) is due mainly to an increase in the facility of O–O bond scission and not to a more favorable complexation equilibrium. The deviation of the kinetically apparent acid dissociation constants ($pK_A = 6.8$ and $pK_B = 10.7$) from the thermodynamically determined acid dissociation constants of 3-$Fe^{III}(H_2O)_2$ ($pK_a = 7.25$) and H_2O_2 ($pK_H = 11.6$)[5i] is not unusual. A deviation of the magnitude observed could be caused by any additional pre-equilibrium step with a K_{eq} of ~2–9.[27]

The Understanding of the Mechanisms of All Oxygen Transfer Reactions Involving Hydroperoxides Requires the Answer to Two Questions: Where Is the Proton in the Transition State and How Is the O–O Bond Broken? These two questions are interrelated. In nucleophilic displacements upon hydroperoxides (YOOH) there can be little doubt that the overall O–O bond cleavage is heterolytic (eq 7). When B: represents secondary or tertiary amines or

$$B: + HOOY \rightarrow BO + YOH \quad (7)$$

hydroxylamines it is found that the reactions are first order in [YOOH] and [B:]. This finding shows that the proton is transferred from the distal to the adjacent oxygen of YOOH without general base (by B:), general acid (by BH^+), or cyclic proton transfer through a second YOOH species.[28] Much the same is true for reactions which involve nucleophilic attack upon YOOH by alkyl sulfides and I^-.[29] Do these reactions occur by stepwise dissociation of YO^- followed by proton transfer in a bimolecular reaction (eq 8a) or within the solvent cage (eq. 8b), or is there back bonding of the proton and its intramolecular transfer in a three-center reaction (eq 9)? The reaction of eq 8a is unlikely for in the case where B: is a tertiary amine or an alkyl

$$B: + HOOY \rightarrow BOH^+ + YO^- \quad (8a)$$

$$B: + HOOY \rightarrow \{BOH^+\ ^-OY\} \rightarrow BO + YOH \quad (8b)$$

$$B: + HOOY \rightarrow \{B\cdots H\cdots O\cdots Y\} \rightarrow BO + YOH \quad (9)$$

sulfide, BOH^+ represents the very acidic protonated *N*-oxide or sulfoxide and YO^- a very basic alkoxide. In the solvent of the study (*t*-BuOH) these species are unstable. This material is presented to impress the reader with the fact that the position of the proton in the transition state, in the much more complicated case of the reaction of hydrogen peroxide with iron(III) porphyrins, is not a trivial question.

We have previously studied the oxidation of *meso*-(tetraphenylporphinato)chromium(III) chloride,[12b] iron(III) chloride,[12c] manganese(III) chloride,[12d,f] and cobalt(III) chloride[12i] (i.e., (TPP)Cr^{III}Cl, (TPP)Fe^{III}Cl, (TPP)Mn^{III}Cl, and (TPP)Co^{III}Cl) with percarboxylic acids and alkyl hydroperoxides in organic solvents. The oxygen–oxygen bond scission for reactions of the various tetraphenylporphyrin metallo(III) chlorides with percarboxylic acids was shown to involve heterolytic O–O bond scission to yield the corresponding carboxylic acid and a $2e^-$ oxidized metal–oxo porphyrin. Plots of the log of the second-order rate constants for the reaction of each metallo(III) tetraphenylporphyrin chloride with percarboxylic acid (YOOH) vs. the pK_a of the carboxylic acid (YOH) departing groups were found to be linear (example, for the formation of iron(IV)–oxo tetraphenylporphyrin π-cation radical from (TPP)Fe^{III}Cl, eq 10).

$$(TPP)Fe^{III}Cl + YOOH \rightarrow (^{+\bullet}TPP)Fe^{IV}O + YOH \quad (10)$$

With TPPCr^{III}Cl, the log of the second-order rate constants for oxygen transfer, when YOOH = alkyl hydroperoxides, could be plotted on the same line as used for percarboxylic acids with use of the pK_a values of YOH = alcohols derived from the hydroperoxides. The constancy of the linear free-energy relationship is in accordance with heterolytic O–O bond scission for the reaction of both percarboxylic acids and alkyl hydroperoxides with (TPP)Cr^{III}Cl. For the reaction of percarboxylic acids and alkyl hydroperoxides with (TPP)Fe^{III}Cl, (TPP)Mn^{III}Cl, (TPP)Mn^{III}(imidazole)$_n$,[12f] and (TPP)Co^{III}Cl, the linear free-energy plots of log k vs. pK_{YOH} exhibited marked breaks to smaller slope at certain values of pK_{YOH}. This change of β_{lg} would be provided by a change of the mechanism of O–O bond cleavage from heterolytic to homolytic for the more weakly acidic alkyl hydroperoxides. The solvent employed with (TPP)Cr^{III}Cl and (TPP)Mn^{III}(imidazole)$_n$ was CH_2Cl_2 while with (TPP)Co^{III}Cl the solvent was $CHCl_3$ and with (TPP)Fe^{III}Cl the solvent was CH_3OH.

Modes of O–O Bond Cleavage in the Transfer of an Oxygen by Hydrogen Peroxide Species to 3-$Fe^{III}(H_2O)$ and 3-Fe^{III}(OH). Several possible transition states are considered for each of the three reaction paths (Scheme II) deduced from the log k_{ly} vs. pH profile (Figure 8) and from the dependence of k_2 on buffer concentration at various pH values. At a pH <5 ($k_{ly} = k_{(A)}$ in eq 6) the reaction is pH independent, with k_a being the second-order rate constant for the overall process. The transition state for the mechanism in this pH range (TS_1) is composed of the components 3-$Fe^{III}(H_2O)$ and H_2O_2. (A number of hypothetical transition-state structures are considered in the present paper. The cartoons representing these states are drawn with ground-state bonds intact. The bonds undergoing cleavage are indicated. This representation is useful since one need not indicate in the cartoon if bond breaking is homolytic or heterolytic.) Three kinetically equivalent structures for TS_1 may be considered (Scheme III). These cannot be differentiated for it is never possible to determine the position of a proton in a transition state by kinetic methods. The first, TS_1A, is derived from the complex 3-$Fe^{III}(H_2O)(H_2O_2)$ (eq 11) and the second TS_1B from H_3O^+ and 3-$Fe^{III}(H_2O)$ and HOO^- (eq 12). From eq 12 there follows eq 13 where K_H and K_z represent the

$$v = k_m[3\text{-}Fe^{III}(H_2O)_2][(H_2O_2)] \quad (11)$$

$$v = k_n[3\text{-}Fe^{III}(H_2O)_2][HO_2^-][H_3O^+] \quad (12)$$

(27) (a) Bruice, T. C.; Schmir, G. L. *J. Am. Chem. Soc.* **1959**, *81*, 4552. (b) Bruice, T. C.; Benkovic, S. J. *Bioorganic Mechanisms*; W. A. Benjamin: New York, 1966; Vol. I, p 13.
(28) Ball, S.; Bruice, T. C. *J. Am. Chem. Soc.* **1980**, *102*, 6498.
(29) Bruice, T. C.; Noar, J. B.; Ball, S. S.; Venkataram, U. V. *J. Am. Chem. Soc.* **1983**, *105*, 2462.
(30) Bruice, T. C.; Donzel, A.; Huffman, W.; Butler, A. R. *J. Am. Chem. Soc.* **1967**, *89*, 2106.

Scheme II

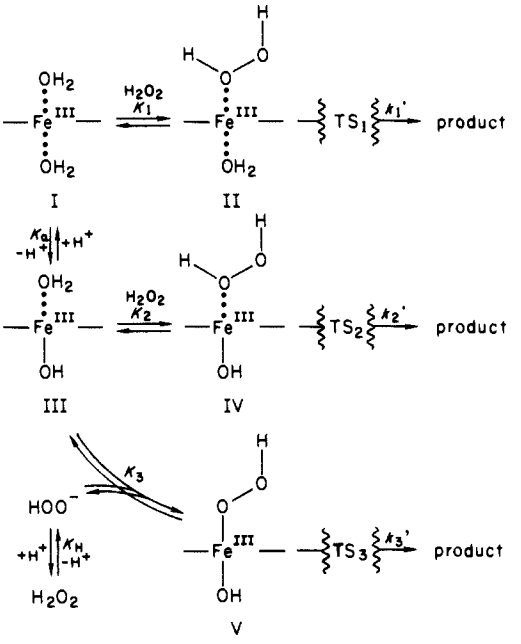

Scheme III

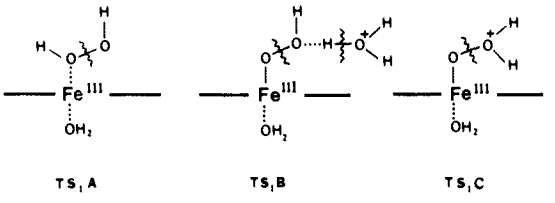

Scheme IV

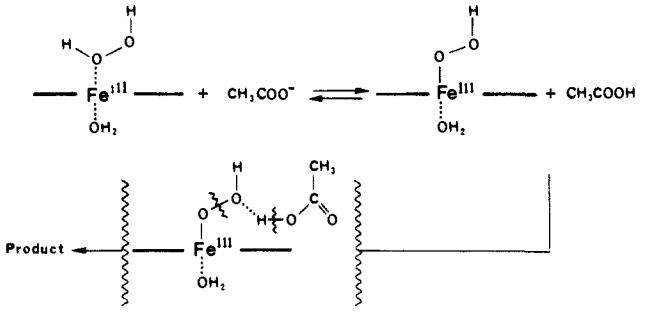

acid dissociation constants of H_2O_2 and H_3O^+, respectively. From eq 11 and 13 one obtains $k_n = k_m K_z/K_H$. With $k_m = 44\ M^{-1}\ s^{-1}$ from the log k_{ly} vs. pH profile (Table I), k_n may be calculated

$$v = (k_n K_H/K_z)[3\text{-}Fe^{III}(H_2O)][H_2O_2] \quad (13)$$

to equal $\sim 10^{15}\ M^{-2}\ s^{-1}$. The third-order rate constant k_n is the product of an equilibrium constant for complexation of 3-$Fe^{III}(H_2O)_2$ with HO_2^- to yield 3-$Fe^{III}(H_2O)(HO_2)$ and a second-order rate constant for reaction of H_3O^+ with this species. It is reasonable to assume that complexing of HO_2^- to the positively charged iron(III) moiety could be associated with an equilibrium constant $\geq 10^6\ M^{-1}$. In that case, the rate constant for the H_3O^+-catalyzed peroxide O–O bond scission within the 3-$Fe^{III}(H_2O)(HO_2)$ complex to yield a higher valent iron–oxo porphyrin would be characterized by a rate constant of $\leq 10^9\ M^{-1}\ s^{-1}$. On this basis both TS_1A and TS_1B are competent (Scheme III). However, TS_1B involves general acid catalysis by the oxygen acid H_3O^+. General catalysis (Scheme IV) could not be observed with the oxygen acid/oxygen base buffers $ClCH_2COOH/ClCH_2COO^-$ or CH_3COOH/CH_3COO^-. This provides a strong argument against TS_1B. In separate experiments it has been determined that the equilibrium constant for the complexation of the iron(III) porphyrin by $CH_3CO_2^-$ is about 1 M^{-1}. Since the $[CH_3CO_2^-]$ used in the buffer dilution experiments ranged from 0.01 to 0.1 M the lack of observation of $CH_3CO_2^-$ catalysis cannot be attributed to a compensating inhibition of rate due to $CH_3CO_2^-$ ligation. This also must be true of the more weakly basic $ClCH_2CO_2^-$. The kinetically equivalent transition-state TS_1C represents specific acid catalysis of the decomposition of 3-$Fe^{III}(H_2O)(HO_2)$. There are no apparent arguments which can eliminate the kinetic competency of TS_1C. We conclude that the transition state associated with the reaction of the iron(III) porphyrin with H_2O_2, in the acidity insensitive range between pH 1 and 5, is represented by TS_1A or TS_1C. The mechanism of O–O bond cleavage in TS_1C must be heterolytic since H_2O is the only possible leaving group. In the case of TS_1A the mechanism may be homolytic (eq 14) or heterolytic (eq 15). (Where the $^{\bullet+}$3-Fe^{IV} moiety represents the iron(IV)–oxo porphyrin π-cation radical which would be formed directly by O–O bond heterolysis.[12e,h]). In considering the heterolytic mechanisms, formation of H_2O may

Scheme V

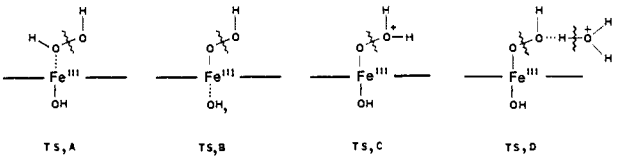

$$TS_1A \rightarrow \{3\text{-}Fe^{IV}(H_2O)OH \cdot OH\} \rightarrow {}^{\bullet+}3\text{-}Fe^{IV}(H_2O)O + H_2O \quad (14a)$$

$$\{3\text{-}Fe^{IV}(H_2O)OH \cdot OH\} \rightarrow 3\text{-}Fe^{IV}(H_2O)OH + HO\bullet \quad (14b)$$

$$TS_1A \rightarrow \{{}^{\bullet+}3\text{-}Fe^{IV}(H_2O)OH\ \bar{O}H\} \rightarrow {}^{\bullet+}3\text{-}Fe^{IV}(H_2O)O + H_2O \quad (15a)$$

$$\{{}^{\bullet+}3\text{-}Fe^{IV}(H_2O)OH\ \bar{O}H\} \rightarrow {}^{\bullet+}3\text{-}Fe^{IV}(H_2O)OH + HO^- \quad (15b)$$

occur after O–O bond cleavage by proton transfer within the solvent cage as shown in eq 15a, by a three-center concerted 1,2-proton shift as depicted in eq 9, or through a spectator[31] H_2O solvent molecule. These three different possibilities for proton transfer in a mechanism involving O–O bond heterolysis and formation of H_2O as a leaving group cannot be differentiated.

The second plateau in the log k_{ly} vs. pH profile of Figure 8 (pH $\sim$7 to 8) represents a reaction for which the transition state possesses the net composition 3-$Fe^{III}(OH)(H_2O_2)$ (see IV, Scheme II). Four kinetically equivalent transition states TS_2A, TS_2B, TS_2C, and TS_2D may be considered (Scheme V). On the basis of the anticipated relative basicity of the oxygen atoms ligated directly to iron, TS_2B would be favored over TS_2A, but reaction paths via both structures are likely. The discussion of modes of O–O bond scission in regard to TS_1A (eq 14 and 15) applies also to TS_2A, so that either heterolysis or homolysis is allowed. TS_2C is also a likely transition-state structure. To judge the feasibility of a reaction being associated with TS_2D, eq 16 and 17 must be compared. Equation 16 pertains to the formation of TS_2A, while

$$v = k_o[3\text{-}Fe^{III}(OH)][H_2O_2] \quad (16)$$

$$v = k_p[3\text{-}Fe^{III}(OH)][HO_2^-][H_3O^+] \quad (17)$$

eq 17 refers to reaction via transition-state TS_2D. From eq 17 there follows eq 18 where K_H and K_z represent the pK_a's of H_2O_2 and H_3O^+, respectively. From eq 16 and 18 it follows that $k_o = k_p K_H/K_z$ and from the log k_{ly} vs. pH profile (Figure 8 and Table I) $k_o = 1.67 \times 10^3\ M^{-1}\ s^{-1}$. Thus, k_p is required to equal $4 \times 10^{16}\ M^{-2}\ s^{-1}$. The third-order rate constant k_p is the product of a second-order rate constant and the equilibrium constant for complexation of HO_2^- with 3-$Fe^{III}(OH)$. In order for the for-

$$v = (k_p K_H/K_z)[3\text{-}Fe^{III}OH][H_2O_2] \quad (18)$$

(31) Kershner, L. D.; Schowen, R. L. *J. Am. Chem. Soc.* **1971**, *93*, 2014.

mation of TS_2D to be allowed, the equilibrium constant for complexation of HO_2^- to 3-Fe^{III}(OH) would have to be $\geq 10^7$ M^{-1}. A value smaller than this would require the rate constant associated with TS_2D to exceed diffusion control. Spectrophotometric titration of 3-Fe^{III}(OH) to pH 14 shows no change in the Soret absorbance, indicating that complexing of a second HO^- moiety to provide 3-$Fe^{III}(OH)_2$ is very endergonic. Though the conjugate acid of HO_2^- is of lower pK_a than that of HO^-, HOO^- possesses a sizable α effect[30] so that these two oxy bases are comparable as nucleophiles. If HO^- shows no detectable propensity to complex with iron(III) porphyrin which is already ligated to an HO^- species, then ligation by HOO^- would not be expected to be highly exergonic. In separate experiments,[12e] carried out in the aprotic solvent CH_2Cl_2, using (*meso*-tetramesitylporphinato)iron(III) methoxide (5-$Fe^{III}(OCH_3)$), it has been found that the addition of 1 equiv of CH_3O^- does not alter either the Soret band nor the $1e^-$ oxidation potential of the metalloporphyrin. Thus, even under the favorable conditions of aproticity, the formation of 5-$Fe^{III}(OCH_3)_2$ from 5-$Fe^{III}OCH_3$ plus CH_3O^- is endergonic. From these considerations the equilibrium constant for complexation of HOO^- with 3-Fe^{III}(OH) could not approach 10^7 M^{-1} but is must likely smaller than 1.0 M^{-1}. A reaction passing through TS_2D is not possible.

The most rapid reaction of hydrogen peroxide with the catalyst occurs at the highest pH values and is characterized kinetically as the plateau rate above pH 11. The rate constant k_c (eq 4) which equals k_3K_3 (cf. eq 6) refers to the reaction of 3-Fe^{III}(OH) with HOO^- (Scheme II). Only the single transition-state structure TS_3 is to be considered. Catalysis is not observed with either CO_3^- or HO^-. From the structure of TS_3, O–O bond scission may be either heterolytic or homolytic.

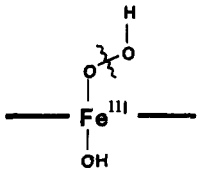

TS_3

Buffer Catalysis Was Only Observed in the pH Region of the Second Plateau of the log k_{1y} vs. pH Profile. Catalysis by the buffer pairs (2,4,6-collidine·HCl)/(2,4,6-collidine), $(H_2PO_4^-)$/(HPO_4^{2-}), and (HCO_3^-)/(CO_3^{2-}) was investigated. Though catalysis by both the sterically hindered 2,4,6-collidine and its conjugate acid was observed, phosphate and carbonate buffer species provided only a slight negative effect upon k_2. The inhibition of the reaction by phosphate and carbonate buffers is presumably caused bycompetitive ligation of the metalloporphyrin by the buffer anions. The reported catalytic effects of phosphate buffers[5g,i,8] on the reaction of hydrogen peroxide with hemins in water are probably due to their influence on the aggregation and dimerization equilibria of the ferric porphyrins employed in those studies. As shown herein, one need not be concerned with these problems when employing 3-Fe^{III}.

With collidine free base the calculated values for the general base catalyzed rate constant (k_B) were of the same order of magnitude as the ones reported by Traylor, Lee, and Stynes using hemins in methanol as solvent.[5m] It is impossible to compare the values of k_{1y}, from the present study, to the nonbuffer catalyzed rate constants of these authors. In the aforementioned investigation, intercepts of plots of determined second-order rate constants vs. buffer concentration (at undetermined acidity) represent rate constants in methanol at unknown acidities, whereas in the present study the intercepts provide second-order rate constants (k_{1y}) at given acidities. Though we show that catalysis by the species 2,4,6-collidine·H^+ and 2,4,6-collidine are comparable, Traylor and co-workers do not report 2,4,6-collidine·H^+ catalysis in methanol solvent. The observation of catalysis by merely the single 2,4,6-collidine/2,4,6-collidine·H^+ buffer pair is not sufficient to establish the phenomenon of general catalysis. To do so requires

Scheme VI

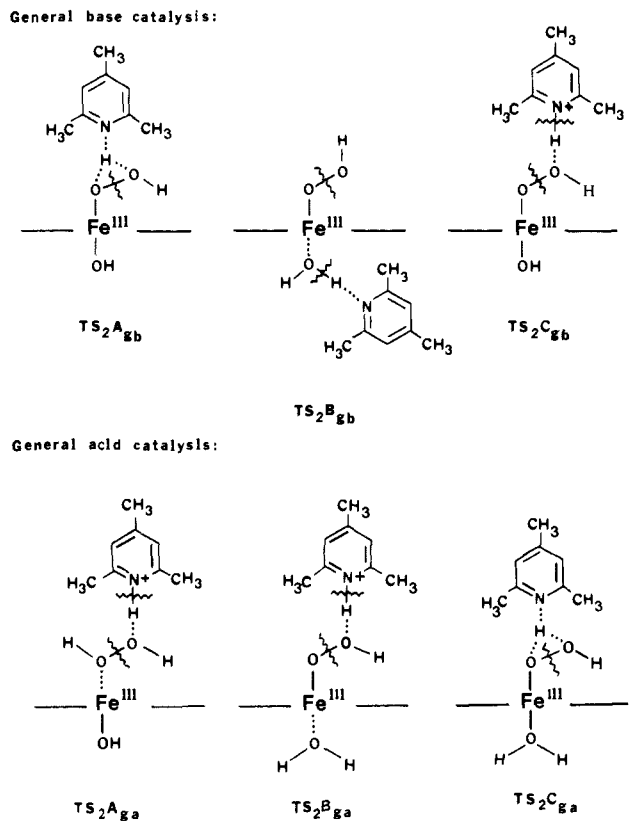

in future studies that other sterically hindered acid/base pairs also show catalytic properties in a ferric porphyrin/H_2O_2 system. With this in mind, and after the fashion of Traylor and co-workers,[5m] we do treat the collidine buffer effect as though it were attributable to general catalysis.

The values of $\Delta G^{\ddagger}$ for collidine and collidine·H^+ catalysis differ by less than 1.0 kcal M^{-1}. Conceivable transition-state structures for the operation of general catalysis by collidine and collidine·H^+ are represented in Scheme VI. This scheme contains three transition-state structure for collidine general base catalysis (TS_2A_{gb}, TS_2B_{gb}, and TS_2C_{gb}) and three transition-state structures for collidine·H^+ general acid catalysis (TS_2A_{ga}, TS_2B_{ga}, and TS_2C_{ga}).

The transition states TS_2A_{gb} and TS_2C_{ga} represent spectator[31] general base catalysis in which the base species involves itself with proton transfer concerted with heterolytic O–O bond scission. In TS_2B_{gb} the general base catalyst removes a proton from ligated water to increase the electron density on iron thereby assisting the latter in the heterolytic or homolytic O–O bond scission. In the instance of the reaction of imidazole ligated (*meso*-tetraphenylporphinato)manganese(III) with alkyl hydroperoxides (solvent CH_2Cl_2), it has been established that an additional imidazole plays the role of catalyst by way of hydrogen bonding to the proton of the imidazole ligand (**6**).[12h] The transition state TS_2B_{gb} also resembles the "proximal base hydrogen bonding" mechanism which has been proposed by a number of workers for peroxidase enzymes.[9b,32] The mechanism associated with transition state TS_2C_{gb} represents general acid catalysis but, since its net composition is identical with that of TS_2A_{gb} and TS_2B_{gb}, it is detected as a collidine base catalyzed process. In considering the plausibility of TS_2C_{gb}, the reader is referred to eq 19, 20, and 21 (where K_H and K_c are the acid dissociation constants of H_2O_2 and collidine·H^+). From eq 19 and 20 it follows that k_q =

(32) (a) Schonbaum, G. R.; Lo, S. *J. Biol. Chem.* **1972**, *247*, 3353. (b) Peisach, J. *Ann. New York Acad. Sci.* **1975**, *244*, 187. (c) Schonbaum, G. R. *Annu. Rev. Biochem.* **1976**, *45*, 861. (d) Nappa, M.; Valentine, J. S.; Snyder, P. A. *J. Am. Chem. Soc.* **1977**, *99*, 5799.

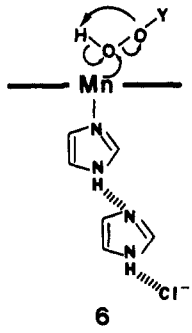

6

$$v = k_q[\text{3-Fe}^{III}(OH)][H_2O_2][\text{collidine}] \quad (19)$$

$$v = k_r[\text{3-Fe}^{III}(OH)][HO_2^-][\text{collidine}\cdot H^+] \quad (20)$$

$$v = (k_r K_H/K_c)[\text{3-Fe}^{III}(OH)][H_2O_2][\text{collidine}] \quad (21)$$

k_rK_H/K_c, and from Figure 7 the value of the experimentally determined collidine base rate constant ($k_B = k_q$) is 8.2×10^4 M^{-2} s^{-1}. Therefore, k_r is required to be minimally 10^9 M^{-2} s^{-1} for TS_2C_{gb} to be a competent transition-state structure. Defining K_s as $[\text{3-Fe}^{III}(OH)(HO_2)]/[\text{3-Fe}^{III}(OH)][HO_2^-]$ there follows eq 22 and 23. Inspection of eq 23 shows that in order for the rate of the reaction involving TS_2C_{gb} to not exceed diffusion control, and

$$v = 10^9[\text{3-Fe}^{III}(OH)][HO_2^-][\text{collidine}\cdot H^+] \quad (22)$$

$$v = (10^9/K_s)[\text{3-Fe}^{III}(OH)(HO_2^-)][\text{collidine}\cdot H^+] \quad (23)$$

thereby to be incompetent, it is necessary that K_s is not smaller than 1 M^{-1}. On the basis that 1.0 M HO^- brings about no change in the spectrum of 3-Fe^{III}(OH) and ligation by HO^- and HOO^- should be comparable (see discussion of TS_2D), the mechanism involving TS_2C_{gb} does not appear likely. This transition state has been favored by other authors.[5m] The rate constant for the reaction proceeding via TS_2A_{ga} is that determined experimentally as k_{BH^+} (2.0×10^4 M^{-2} s^{-1}; Figure 7) so that this mechanism is competent.

The influence of general base removal of the ligand proton in TS_2B_{gb} upon the rate of O–O bond scission may be evaluated from the knowledge that the complete removal of the ligand proton via specific base catalysis (in going from 3-$Fe^{III}(H_2O)(HOO)$ to 3-Fe^{III}(OH)(HOO)) at the upper plateau is associated with an increase in k_{1y} of 60, while the ratio of k_B (for collidine buffer catalysis)/k_{1y} (for reaction of 3-$Fe^{III}(H_2O)$(HOO)) is 50 M^{-1}. This means that 1.0 M collidine free base acting as a general base catalyst in the intermediate pH range—ignoring changes in the solvent composition—would give a rate of reaction for 3-Fe^{III}-(H_2O)(HOO) which is about that for the spontaneous reaction of 3-Fe^{III}(HO)(HOO) at high pH. Due to the limited miscibilities of collidine/water mixtures, reactions at 1 M collidine could not be carried out. In principle, however, this mechanism would implicate that at [free collidine] > 2.0 M the rate of the general base catalyzed reaction would be larger than the rate of the upper plateau of the log k_{1y} vs. pH profile, where removal of the proton of ligated water is complete. This cannot be so, because catalysis involving TS_2B_{gb} merely represents concerted removal of this proton by the general base, and the observed rate at the upper plateau must be the limiting value for the rate associated with this transition state. The transition state TS_2B_{gb} may be discounted. The very same considerations rule out a mechanism whereby collidine general base removes a proton of the ligated H_2O_2. The only collidine general base mechanism which would allow a rate larger than the one observed at the upper plateau is the mechanism involving spectator[31] catalysis of 1,2-proton transfer by collidine free base (TS_2A_{gb}). The transition state TS_2C_{ga} represents the same spectator general base catalysis as does TS_2A_{gb} but involves as substrate 3-$Fe^{III}(H_2O)(H_2O_2)$ rather than 3-Fe^{III}(HO)(H_2O_2). Equation 24 represents the rate law

$$v = k_s[\text{3-Fe}^{III}(OH)(H_2O_2)][\text{collidine}\cdot H^+] \quad (24)$$

for collidine·H^+ catalyzed oxygen transfer within the 3-Fe^{III}-

Table III. Transition-State Structures for Non-Buffer-Catalyzed Reactions of Hydroperoxide and Iron(III) Porphyrin Species. The Possible Modes of O–O Bond Cleavage (Homolytic and/or Heterolytic [eq 14 and 15] and Heterolytic) Are Indicated

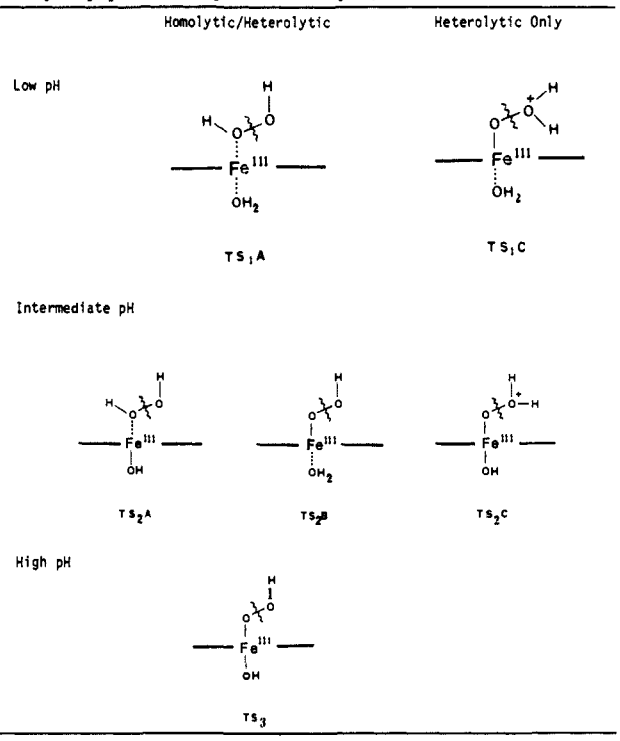

(OH)(H_2O_2) complex (TS_2A_{ga}). From eq 24 there follows in eq 25 the rate law for the mechanism involving TS_2C_{ga} (where K_c

$$v = \frac{k_s K_a^-}{K_c}[\text{3-Fe}^{III}(H_2O)(H_2O_2)][\text{collidine}] \quad (25)$$

is the acid dissociation of collidine·H^+ and K_a the acid dissociation constant for 3-$Fe^{III}(H_2O)(H_2O_2)$ going to 3-Fe^{III}(OH)(H_2O_2)). The value of pK_c is 7.47 and pK_a^- may be taken as identical with that of 3-$Fe^{III}(H_2O)_2$ dissociating to 3-Fe^{III}(OH)(H_2O) which is 7.25. Since $pK_a^- = pK_c$ the rate constant k_sK_a/K_c is approximated by the experimentally determined general acid rate constant (k_{BH^+}) and TS_2C_{ga} represents also a kinetically competent mechanism. The acceptable mechanisms for collidine general base and general acid catalysis (i.e., TS_2A_{gb}, TS_2A_{ga}, TS_2B_{ga}, and TS_2C_{ga}) have in common H_2O as the leaving group and would involve heterolytic O–O bond scission.

Concluding Remarks Concerning Mechanisms of Oxygen Transfer. In the present study we have shown that there are three non-buffer-catalyzed reaction pathways, depending upon pH, for the oxidation of an iron(III) porphyrin by hydrogen peroxide (Scheme II). The composition of the transition states for all three reaction paths is kinetically defined. From the compositions a number of kinetically equivalent transition-state structures may be drawn. Some of the structures have been dismissed as being incompetent. Those that remain for the three reaction paths which do not include buffer species are shown in Table III. We have previously presented evidence[12c] which may be interpreted to show that the reaction of hydroperoxides with iron(III) tetraphenylporphyrin in methanol involves homolytic O–O bond scission. If this should be true in water then TS_1C and TS_2C may be dismissed. The acidity independent rate of reaction at low pH is comparable to that of H_2O_2 with (tetraphenylporphinato)iron(III) chloride in pure methanol.

In Table IV are listed the possible transition-state structures for 2,4,6-collidine·H^+ and 2,4,6-collidine catalysis. Since the four structures require H_2O as the leaving group, the reactions must involve heterolytic O–O bond scission. The structures TS_2A_{gb} and TS_2C_{ga} represent the same mechanisms for proton transfer, and since TS_2A_{gb} is the only competent structure for 2,4,6-collidine

Table IV. Transition-State Structures for 2,4,6-Collidine·H^+ and 2,4,6-Collidine Catalyzed Reactions of Hydrogen Peroxide and Tetraphenylporphyrin–Iron(III) Species. All Competent Reactions Involve Heterolytic O–O Bond Scission

2,4,6-Collidine Catalysis

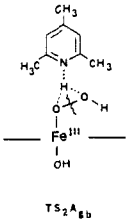

TS_2A_{gb}

2,4,6-Collidine·H^+ Catalysis

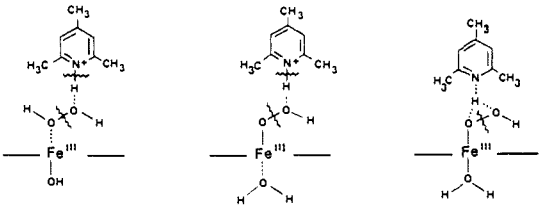

TS_2A_{ga} TS_2B_{ga} TS_2C_{ga}

free-base catalysis, it might be argued that of the three possible transition states for collidine·H^+ catalysis the structure TS_2C_{ga} should be favored. On the basis of the present study, the spectator 1,2-prototropic shift with partially concerted O–O bond heterolysis (as seen in TS_2A_{gb} and TS_2C_{ga}) represents the best mechanism for the peroxidase enzymes. The inability to detect general catalysis with the carboxyl acid–base pairs $ClCH_2CO_2H/ClCH_2CO_2^-$ and $CH_3CO_2^-/CH_3CO_2H$, as compared to the ability to observe such catalysis with the 2,4,6-collidine tertiary amine acid–base pair, could be due to electrostatic repulsion and attraction in the transition states.[33] If in TS_2A_{gb} and TS_2C_{ga} electron transfer from iron to oxygen and O–O bond heterolysis were advanced, a partially negative charge would reside on the leaving oxygen and a partially positive charge on the collidine nitrogen. Attraction between the negative and positive charges would serve to stabilize the transition state. On the other hand, such a transition state with a negatively charged catalytic base would not be so stabilized and could involve charge repulsion and destabilization of the transition state.

Competition of ABTS and H_2O_2, as Oxidizable Substrates, for the Higher Valent 3-Iron–Oxo Species Generated by Oxygen Transfer from H_2O_2 and HOO^-. The yield of $ABTS^{\bullet+}$, which is approximately 100% below pH 2, drops drastically in the intermediate pH region, asymptotically approaching 20% at pH values above 9. This is due to ABTS oxidation being in competition with the oxidation of hydrogen peroxide. Hydrogen peroxide oxidation is catalyzed by catalase (Scheme I) and at high pH by a higher valent iron–oxo species derived from EDTA–Fe^{III}.[34] The evolution of O_2, in the reaction of **3**-Fe^{III} aquo species with H_2O_2, was shown by employing an oxygen electrode. The second-order rate constants for oxygen production (k_2) were of the same order of magnitude as the rates of $ABTS^{\bullet+}$ formation at the same pH values and buffer concentrations. This also shows that the rate-determining step precedes the formation of O_2 and $ABTS^{\bullet+}$ and must, therefore, be O–O bond cleavage and the formation of the higher valent iron–oxo porphyrin (Scheme I). The yield of O_2 at pH 8 was about two times greater than at pH 5.2, showing that the percentage yield of O_2 increases as the percentage yield of $ABTS^{\bullet+}$ decreases. The reaction of the higher valent iron–oxo porphyrin with H_2O_2 merits further investigation.

Experimental Section

Instrumentation. UV–vis spectra were measured on a Cary 118C spectrophotometer at 30 °C. ^1H NMR spectra were recorded on a Nicolet NT-300 spectrometer (300 MHz). Chemical shifts are reported in ppm (δ) downfield from tetramethylsilane (external standard). Cyclic voltammetry was carried out with a three-electrode potentiostat (Bioanalytical Systems Model CV-27 Voltammograph) connected to a Houston Instruments Model 100 x–y recorder. The electrochemical cell was equipped with a Bio-analytical Systems glassy carbon electrode, a platinum flag auxiliary electrode, and an Ag/AgCl reference electrode filled with aqueous tetraethylammonium chloride adjusted to 0.00 V vs. a saturated calomel electrode. Elemental analyses were carried out by Galbraith Laboratories, Inc., Knoxville, TN. Mass spectra were taken at the University of California, San Francisco, Mass Spectrometry Facility and at the Department of Chemistry, University of California, Riverside. For thin-layer chromatography reversed phase KC_{18} plates (Whatman) were used. HPLC separations were attempted with a Perkin-Elmer Series 10 Liquid Chromatograph, interfaced with a Hewlett Packard 3391A integrator on a Whatman Partisil 5 ODS-3 column. Measurements of pH were performed by using a Beckman 4500 digital pH meter with a Beckman standard combination pH electrode or a Radiometer model pHM 26 with a Metrohm electrode. Spectrophotometric titrations of pK_a values were carried out with a CARY 15 spectrophotometer equipped with a thermostated cell (path length 3.387 cm) fitted with a magnetic stirrer and a glass electrode. Absorbance vs. time measurements were recorded on a Perkin-Elmer 553 fast-scanning spectrophotometer equipped with a constant temperature cell holder at 30 °C. Rapid mixing experiments were carried out on a Durrum stopped-flow spectrophotometer thermostated at 30 °C interfaced to a North Star Computer equipped with OLIS 3820 data acquisition and processing software (On-Line Instruments Systems, Inc.). Calculations of first-order rate constants, least-squares slopes, titration curves, and pH–rate profiles were performed on a Hewlett-Packard 9825A desk computer equipped with a 9864A digitizer and plotter using programs available in our laboratory. Oxygen evolution was measured wth a Yellow Springs Instrument Co. Inc., YSI Model 53 Oxygen Monitor (5331 oxygen electrode).

Materials. Deionized, double-glass distilled water was used for all experiments. All chemicals were of the best available purity. Sodium tetrakis(*p*-sulfonatophenyl)porphyrin (**4**) was from Strem Chemicals. 2,2′-Azinobis(3-ethylbenzthiazoline)sulfonic acid(6) diammonium salt (ABTS) was obtained from Sigma. 2,4,6-Collidine was purchased from Aldrich and was shown to be ~100% pure by gas chromatography. 2,6-Dimethylbenzaldehyde was from Chemical Services, Inc., Hanover, NJ. All buffer and salt solutions were extracted with 0.01% dithizone in carbon tetrachloride (below pH 7) or passed over a column of Chelex 100 to remove any heavy metal contamination. The cuvettes were regularly soaked in 1% EDTA overnight and washed extensively with doubly distilled water. The concentration of hydrogen peroxide (Mallinckrodt 30%) was determined iodometrically.

Syntheses. (5,10,15,20-Tetrakis(2,6-dimethylphenyl)porphinato)zinc(II) (1-Zn^{II}). 2,6-Dimethylbenzaldehyde (14.0 g, 104 mmol), 9.0 mL (130 mmol) of freshly distilled pyrrole, 1.7 g (7.75 mmol) of zinc acetate dihydrate, and 25 mL of pyridine were sealed in a heavy-walled glass reaction bomb and heated in an oven at 185 °C for 65 h. The tarry-black reaction mixture was removed from the flask by repeated washing with acetone. The acetone washes were combined, diluted to 300 mL with more acetone, and placed in the freezer for 8 days. The purple crystalline precipitate was filtered and washed with cold acetone (1.05 g). Concentration and cooling of the mother liquor did not yield any more solid material. The crude product containing a mixture of Zn-porphyrin and Zn-chlorin was dissolved in 150 mL of analytical grade benzene (dried over 4A molecular sieves), a solution of 0.31 g (1.3 mmol) of 2,3-dichloro-5,6-dicyano-1,4-benzoquinone (DDQ) in 25 mL of benzene was added, and the mixture was heated to reflux for 3 h. The solution was vacuum-filtered through a 2 cm layer of neutral alumina (activity 2) on a sintered glass funnel, evaporated to dryness, and chromatographed on a column of neutral alumina (activity 2) with benzene:dichloromethane (96:4). A broad pink band developed which was collected. Evaporation of the solvent and drying overnight under high vacuum yielded 940 mg (4.6%) of shiney purple crystals: UV–vis max (CH_2Cl_2, $c = 6.94 \times 10^{-5}$ M, 2.78×10^{-6} M) 584 (ϵ 2.00×10^3), 548 (2.29×10^4); 510 (3.21×10^3), 483 (sh), 418 (6.41×10^5), 391 nm (4.76×10^4); ^1H NMR (300 MHz, CD_2Cl_2) δ 8.63 (s, 8 H, β-pyrrole-H), 7.57 (t, J = 7.5 Hz, 4 H, *p*-Ph-H), 7.44 (d, J = 7.5 Hz, 8 H, *m*-Ph-H), 1.89 (s, 24 H, *o*-CH_3).

5,10,15,20-Tetrakis(2,6-dimethyl-3-sulfonatophenyl)porphyrin (3). A slurry of 100 mg (0.127 mmol) of 1-Zn^{II} and 15 mL of concentrated

(33) (a) Bruice, P. Y. *J. Am. Chem. Soc.* **1984**, *106*, 5959. (b) Kresge, A. J.; Chen, H. L.; Chiang, Y.; Murrill, E.; Payne, M. A.; Sagatys, D. S. *J. Am. Chem. Soc.* **1971**, *93*, 413. (c) Kresge, A. J.; Chiang, Y. *Ibid.* **1973**, *95*, 803. (d) Ewing, S. P.; Lockshon, D.; Jencks, W. P. *J. Am. Chem. Soc.* **1980**, *102*, 3072.

(34) Walling, C.; Kurz, M.; Schugar, H. J. *Inorg. Chem.* **1970**, *9*, 931.

sulfuric acid was heated to 100 °C for 4 h and left at room temperature for an additional 22 h. The mixture was neutralized with saturated sodium hydroxide solution under cooling, evaporated to dryness under reduced pressure, and extracted exhaustively with methanol. From the evaporated methanolic solution one obtained 120 mg of crude product which was dissolved in 2 mL of water and passed over a cation exchange column (Dowex 50 WX-8, H^+-form). The purple-colored fraction was collected, neutralized with sodium hydroxide, and evaporated to dryness. The solid was dissolved in methanol, filtered, reduced to 2 mL, and chromatographed on a column of Sephadex LH 20 (100 × 5 cm) with methanol. The main fraction, a purple band, was collected, reduced to 2 mL volume, and precipitated with acetone, giving 63 mg (38%) of a dark purple microcrystalline powder: mp >300 °C; mass spectrum (Liquid SIMS positive spectrum, glycerol–thioglycerol [1:1]): m/z 1135 (M + 1), 1113, 1091 (100), 1069, 1047; most abundant peak in isotopic cluster for $C_{52}H_{42}N_4S_4O_{12}Na_4$, 1134.127; laser desorption Fourier transform mass spectra (NH_4Br), m/z 1091, 1069, 1047 (100, M + 1 − 4 Na), 989, 967, 909, 887. ^1H NMR (300 MHz, CD_3OD): δ 8.8–8.5 (m, 8 H, β-pyrrole-H), 8.36 (d, J = 8 Hz, 4 H, p-Ph-H), 7.58–7.50 (m, 4 H, m-Ph-H), 2.344, 2.320, 2.292, 2.259 (4 "s", ca. 1:3:3:1, 12 H, CH_3), 1.882, 1.852, 1.823, 1.796 (4 "s", ca. 1:3:3:1, 12 H, CH_3); UV–vis max (H_2O, c = 2.3 × 10^{-5} M) 633 (ϵ 2200), 580 (6900), 550 (4800), 513 (19 800), 482 (sh, 3100), 413 nm (635 000); R_f (KC_{18}, n-butyl alcohol:H_2O (2% tetrabutylammonium bromide) = 8:2) 0.57, 0.50, 0.35; IR (KBr) 1630, 1180, 1055, 964, 805, 735, 690 cm^{-1}. Anal. Calcd for $C_{52}H_{42}N_4S_4O_{12}Na_4 \times 9H_2O$ (FW = 1297.27): C, 48.15; H, 4.66; N, 4.32; S, 9.89. Found: C, 47.92; H, 4.60; N, 4.29; S, 10.58.

Iron(III) [5,10,15,20-Tetrakis(2,6-dimethyl-3-sulfonatophenyl)-porphyrin] (3-Fe^{III}). **3** (80.2 mg, 0.06 mmol) and $FeSO_4 \times 7H_2O$ (638 mg, 2.3 mmol) in 5 mL of water were heated to reflux for 20 h. During the reaction time the pH was adjusted three times to 5–8 with 1 N sodium hydroxide. The course of the reaction was followed by UV–vis spectroscopy by examining the Soret region of acidified samples. Solid NaOH was added until the pH was 12–13. The brown mixture was chilled and filtered through a glass frit. The solid residue was washed with water and discarded. The filtrate was passed over a column of Dowex 50 WX-8 (H^+-form). The pH of the eluate was adjusted to pH 6 with NaOH and evaporated under reduced pressure. The solid material was dissolved under heating and sonication in 1–2 mL of methanol with 3 drops of 0.1 M HCl added and chromatographed on a column of Sephadex LH 20 (100 × 5 cm) with methanol. Two bands developed, one reddish-brown and one greenish-brown. The eluate was collected in 30-mL fractions and the fractions were pooled according to the appearance of the Soret band in acidic solution. F1, the major fraction, exhibited a Soret band at 393 nm which shifted to 413 nm on basification. The slower travelling material, F2, had a Soret maximum at 413 nm which was pH independent. F1 was rechromatographed under the same conditions. The solid obtained from the evaporated eluate was dissolved in 2 mL of water and precipitated with 150 mL of acetone at 0 °C to yield 20–40 mg (21–44%) of a dark-brown or purple powder: mp >300 °C; ^1H NMR (300 MHz; D_2O/DCl) δ 45.5 (br s, half-width 180 Hz, 8 H, β-pyrrole-H), 10.50 (s, 4 H, m-Ph-H), 9.37 (s, 4 H, p-Ph-H), 4.0-2.0 (2 m, 24 H, o-CH_3); (300 MHz, D_2O/NaOD) δ 80 (br s, half-width 1500 Hz, β-pyrrole-H), 14–13, 13–12 (2 m), 9.5–8.5 (2 m), 3.7–2.0 (several m, o-CH_3). Anal. Calcd for $C_{52}H_{40}S_4O_{12}FeNa_4 \times 0.5SO_4^{2-} \times 16H_2O$ (FW 1527.22): C, 40.89; H, 4.75; N, 3.67; S, 9.45; Fe, 3.66. Found: C, 40.87; H, 4.62; N, 4.18; S, 9.68; Fe, 3.06. UV–vis max (pH 3.25, KH–phthalate) 657 (ϵ 3850), 520 (sh, 4400), 528 (12 200), 505 (10 660), 408 (sh, 94 900), 393 nm (119 800); UV–vis max (pH 9.71, $NaHCO_3$) 585 (sh, ϵ 5600), 560 (sh, 7150), 475 (sh, 14 000), 413 nm (128 300); R_f (KC_{18}, n-butyl alcohol:water [2% tetrabutylammonium bromide] = 8:2) 0.59 and 0.50.

Methods. Buffers were prepared by mixinng appropriate amounts of the acid and base species. The pK_a of collidine was determined (μ = 0.20, 30 °C) by half-neutralization to be 7.47 (pK_a = 7.45 at 25 °C).[35] The kinetics of the reaction of hydrogen peroxide with 3-Fe^{III} were determined by following the increase of absorbance of $ABTS^{\bullet+}$ at 660 nm at 30 °C. The kinetic runs were typically carried out by mixing in quartz cuvettes with 10 mm path length 10–100 μL volumes of a 130–150 × 10^{-6} M solution of 3-Fe^{III} in water, 14 μL 1 × 10^{-2} M hydrogen peroxide in water, and 3.00 mL of an ABTS stock solution (3.5 × 10^{-3} M) of the appropriate pH and buffer concentration (ionic strength was adjusted with sodium nitrate to μ = 0.2077). The final concentrations were usually [3-Fe^{III}] = 4 × 10^{-7}–5 × 10^{-6} M, [H_2O_2] = 4.50 × 10^{-5} M, [ABTS] = 3.37 × 10^{-3} M, μ = 0.20 M, with buffer concentration and pH being the variables. The pH was determined at the completion of each kinetic run, and the results were discounted if initial and final pH values differed by more than 0.03. The experimental curves of A_{660} vs. time were digitized and computer-fitted to calculated pseudo-first-order rate constants.

The rate constants at pH 12 were determined by stopped-flow spectrophotometry ([3-Fe^{III}] = 1.3 × 10^{-7}–1.3 × 10^{-6}, [H_2O_2] = 4.5 × 10^{-5} M, [ABTS] = 3.7 × 10^{-3} M). For these experiments the absorbance vs. time data were analyzed as described under Instrumentation to obtain first-order rate constants.

Acknowledgment. This work was supported by grants from the National Institutes of Health and the National Science Foundation. M.F.Z expresses appreciation to the BASF AG of West Germany for a postdoctoral fellowship. Mass spectral measurements were performed under the auspices of UCSF Mass Spectrometry Facility supported by NIH Division of Research Resource Grant RR 01614 and the Mass Spectral Facility At UCR under the direction of Professor C. L. Wilkins (NIH GM 30604).

Registry No. 1-Zn^{II}, 91947-22-7; 3·4Na, 102575-55-3; 3-Fe^{III}-$(H_2O)_2$·4Na·0.5SO_4, 102588-49-8; 4-$Fe^{III}(H_2O)_2^{3-}$, 70288-08-3; 6(diammonium salt), 30931-67-0; H_2O_2, 7722-84-1; H_2O, 7732-18-5; 2,6-dimethylbenzaldehyde, 1123-56-4; pyrrole, 109-97-7; collidine, 29611-84-5; chloroacetate, 14526-03-5; acetate, 71-50-1; phosphate, 14265-44-2; carbonate, 3812-32-6.

(35) Gero, A.; Markham, J. J. *J. Org. Chem.* **1951**, *16*, 1835.